PART III

SYSTEM SIMULATION

CHAPTER SEVEN

SIMULATION OF THE DSSS TRANSMITTER

7.1 INTRODUCTION AND DESCRIPTION

Simulation of the complete complex DSSS communication system, prior to hardware implementation, in order to evaluate and verify correctness of the theoretical design, is absolutely essential and of inestimable value during the realisation phases of the project. To enhance the operation of the overall system, modifications of the structures as well as fine tuning of certain parameters can be achieved with relatively ease using the simulation platform.

The complete DSSS system employing complex spreading sequences, designed and analyzed in Chapters 4, 5 and 6, was simulated in C++. This chapter presents the results obtained for the transmitter part. Figure 7.1 shows the block diagram of the complete simulation setup. The complete setup consists of a data source supplying random bipolar data, a DSSS modulator that spreads this data with a complex spreading sequence, an AWGN source that provides noise samples to be added to the output of the modulator, a DSSS demodulator, responsible for the demodulation and despreading of the data signal and a BER meter to measure the bit error performance of the system. The spreading sequence length, L, the prime value, r, and samples-per-symbol, sps, are parameters that can be adjusted at the DSSS modulator and demodulator, while the average, μ, and the variance, σ^2, are adjustable parameters in the AWGN source. The last two parameters are used to calibrate the AWGN source to ensure the correct E_b/N_o value required to measure the bit error performance of the system.

The simulated DSSS transmitter is illustrated in Figure 7.2. The results presented are for

the balanced as well as the dual channel QPSK configurations. The results presented show the temporal characteristics (time signals) as well as the the corresponding frequency spectra at different points in the transmitter.

7.2 SIMULATION RESULTS AND DISCUSSION

In this simulation complex spreading sequences were used as discussed in Chapter 3. The real and imaginary parts of a DSB complex spreading sequence, with a length of 121, are shown in Figure 7.3 in (a) and (b), respectively. The unique derived combinations of the real and imaginary parts of the CSS, $C_r - C_i$ and $-C_r - C_i$, discussed previously, are shown in Figure 7.4 in (a) and (b), respectively, with a length of $L = 121$. Figure 7.5, (a) and (b), presents the real and imaginary parts of a SSB CSS, respectively, while Figure 7.6, (a) and (b), presents the unique combinations of the real and imaginary parts of the SSB CSS, $C_r - C_i$ and $-C_r - C_i$, respectively. Both cases are for a spreading sequence length of 121. All of these sequences in Figures 7.3 to 7.6 are filtered by interpolating on the unit circle, as described in [10].

These unique combinations of the real and imaginary parts of the CSS are used in the transmitter for spreading the data signals on the in-phase and quadrature phase branches. The DSB CSS are used for spreading in both the balanced QPSK and normal dual channel QPSK configuration, while the SSB CSS are used only in the balanced QPSK configuration to produce a SSB transmitter output signal. Figure 7.7 shows the in-phase and quadrature phase branch signals in a balanced QPSK configuration spreaded with the unique combinations C_1 and C_2 of the DSB CSS, respectively. Figure 7.8 shows the same two branch signals where the data are spreaded with the unique combinations C_1 and C_2 of the SSB CSS, respectively. Figures 7.9 and 7.10 show the PSD of the spreaded branch signals for the DSB CSS C_1 and C_2 respectively, while Figures 7.11 and 7.12 depict the PSD for same two branch signals for the case of SSB CSS. In Figures 7.13 and 7.14 the time signals of the spreaded branch signals, modulated onto the quadrature carrier, are shown for the DSB and SSB CSS, respectively, while Figures 7.15, 7.16, 7.17 and 7.18 show the PSD of these signals. The final output signal of the transmitter, when using DSB CSS for spreading, is illustrated in Figure 7.19. Only one sideband remains, compared to the DSB case in Figure 7.19, when the SSB CSS are used for spreading on the two branch signals, and is presented in Figure 7.20. In the case

of SSB CSS spreading, the spectra on the two quadrature carriers, are DSB but produces a SSB output signal when they are added. This is because the one branch signal is the Hilbert transform of the other and thus produces a SSB output signal when they are summed.

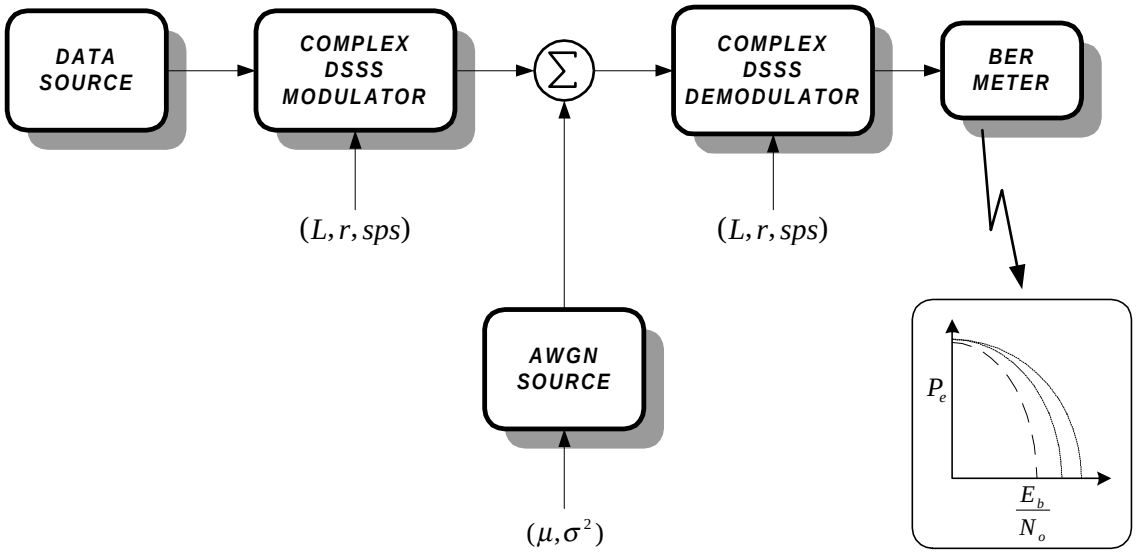

FIGURE 7.1: Block diagram of the complete simulation setup

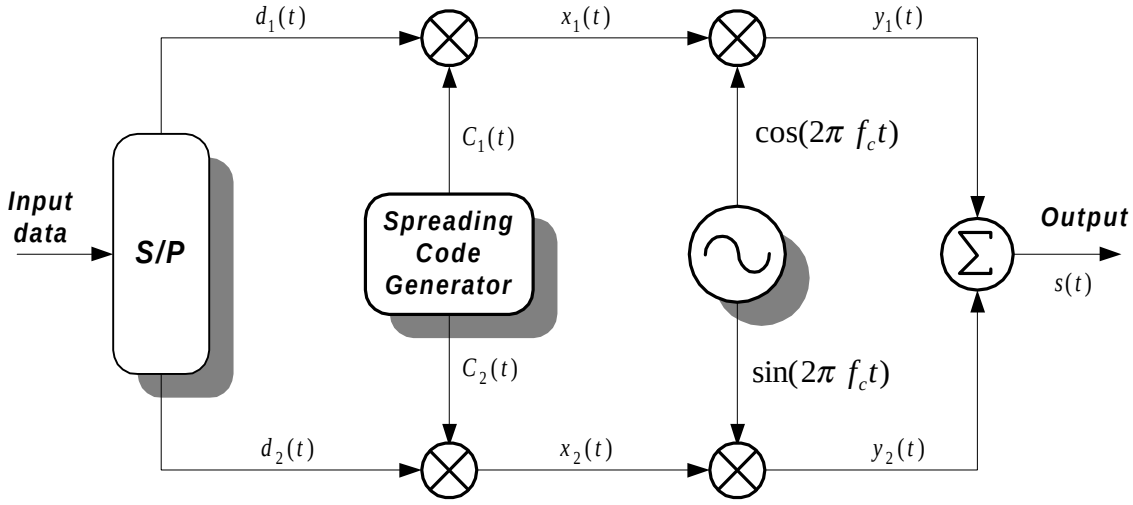

FIGURE 7.2: Block diagram of the transmitter structure used in the simulation

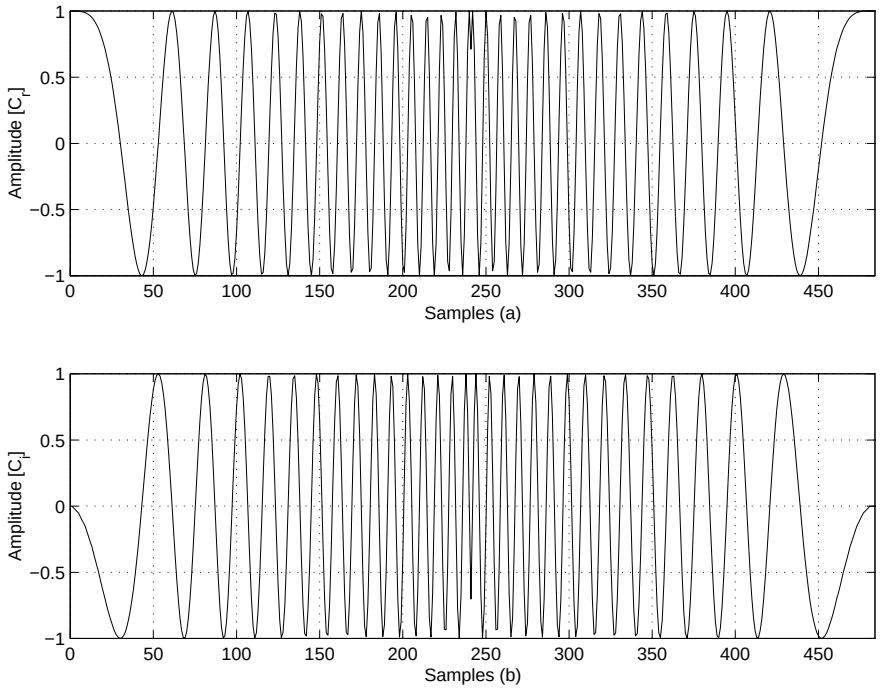

FIGURE 7.3: Real part of the DSB CSS in (a) and imaginary part of the DSB CSS in (b) with L=121, sps=4 and r=1

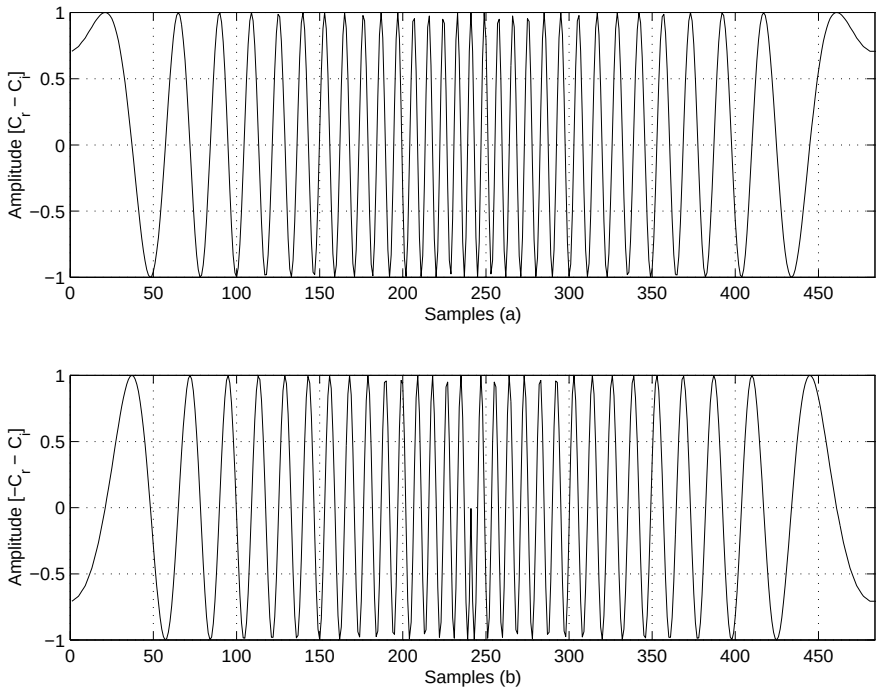

FIGURE 7.4: Unique combinations of the real and imaginary parts of the DSB CSS. $[C_r - C_i]$ in (a) and $[-C_r - C_i]$ in (b) with L=121, sps=4 and r=1

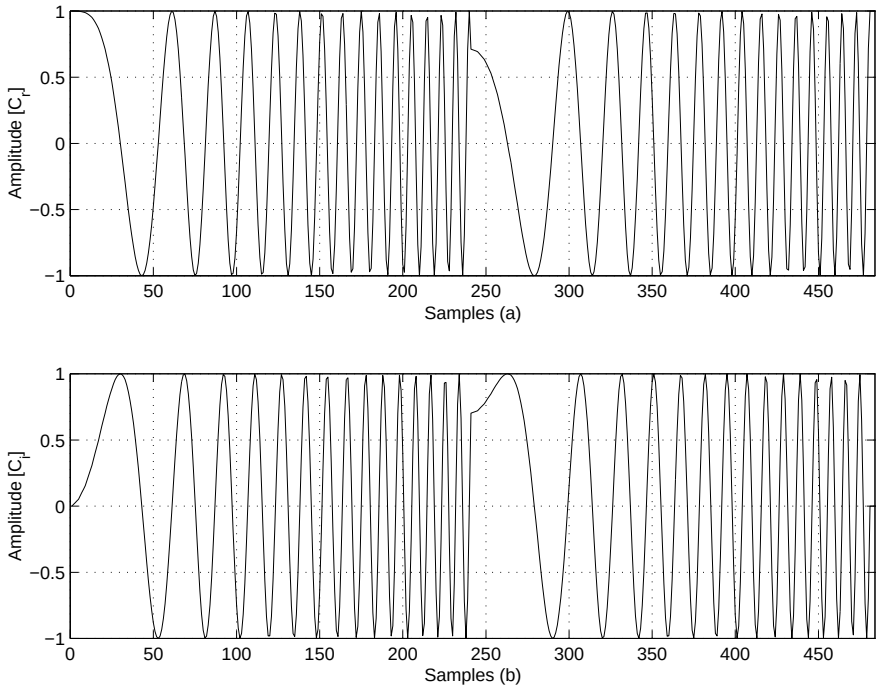

FIGURE 7.5: Real part of the SSB CSS in (a) and imaginary part of the SSB CSS in (b) with L=121, sps=4 and r=1

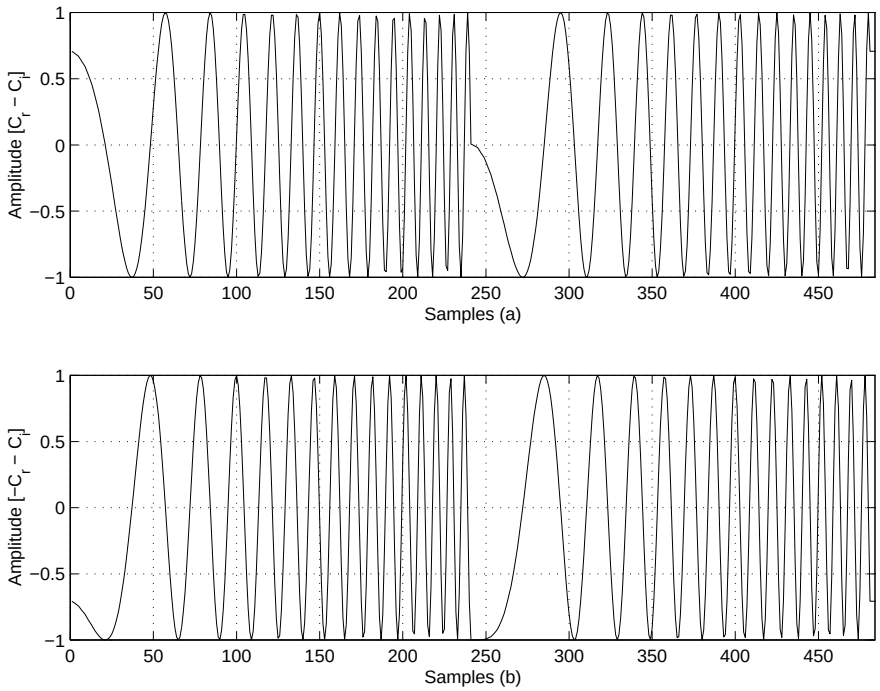

FIGURE 7.6: Unique combinations of the real and imaginary parts of the SSB CSS. $[C_r - C_i]$ in (a) and $[-C_r - C_i]$ in (b) with L=121, sps=4 and r=1

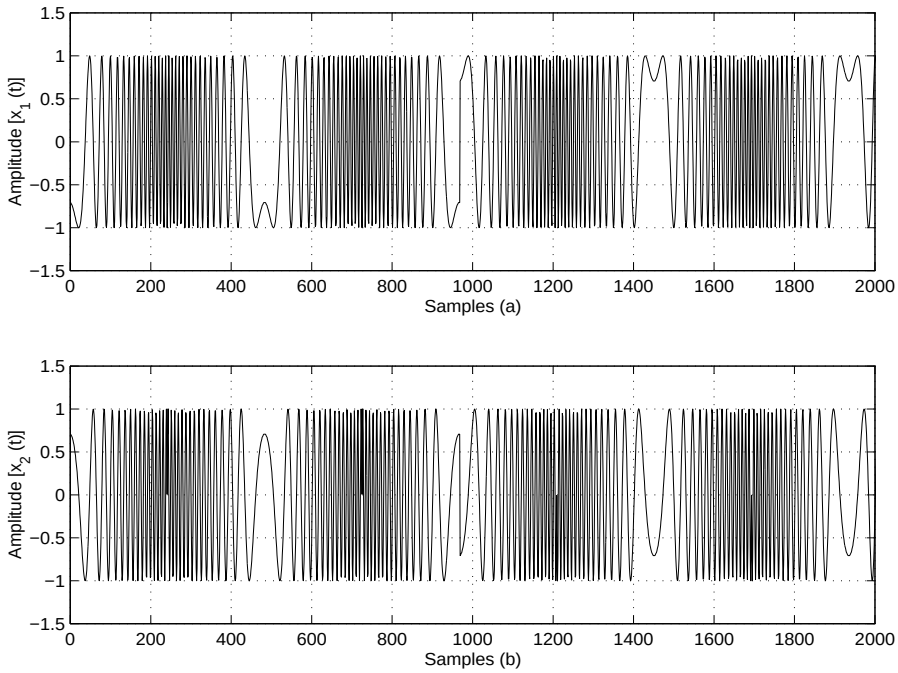

FIGURE 7.7: Data stream on in-phase branch spreaded with DSB CSS combination: $[C_r - C_i]$ in (a) and data stream on quadrature-phase branch spreaded with DSB CSS combination: $[C_r - C_i]$ in (b). (L=121, sps=4 and r=1)

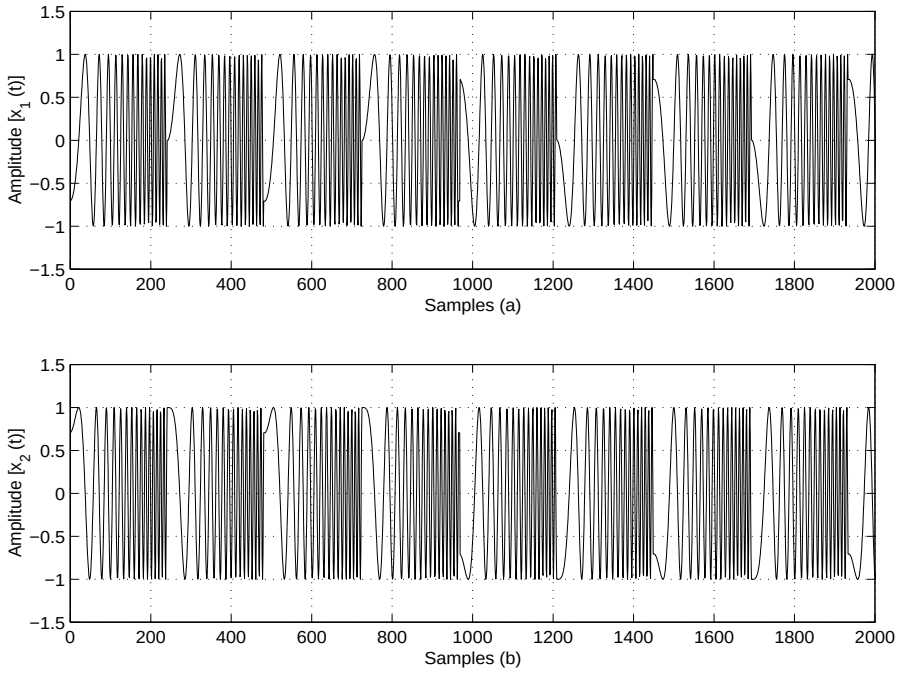

FIGURE 7.8: Data stream on in-phase branch spreaded with SSB CSS combination: $[C_r - C_i]$ in (a) and data stream on quadrature-phase branch spreaded with SSB CSS combination: $[C_r - C_i]$ in (b). (L=121, sps=4 and r=1).

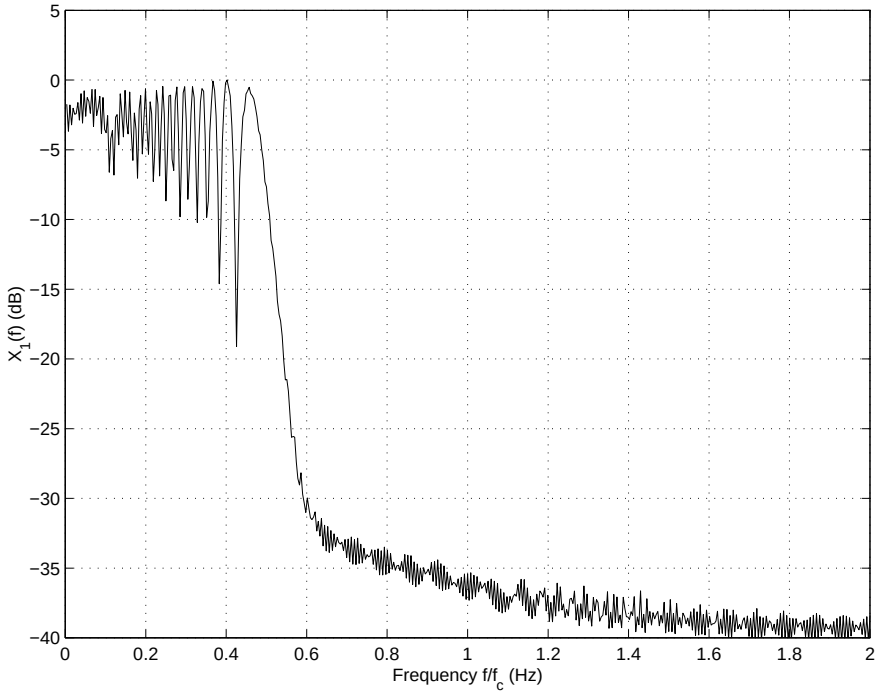

FIGURE 7.9: PSD of the in-phase branch at the transmitter after spreading of the data signal with the DSB complex unique combination spreading code C_1 (L=121,sps=4,r=1).

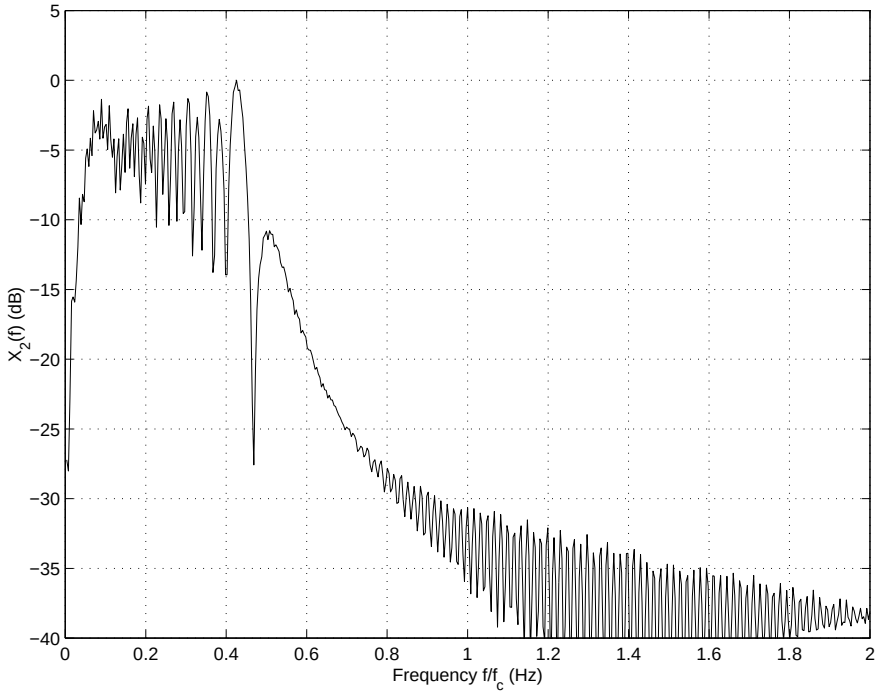

FIGURE 7.10: PSD of the quadrature-phase branch at the transmitter after spreading of the data signal with the DSB complex unique combination spreading code C_2 (L=121,sps=4,r=1).

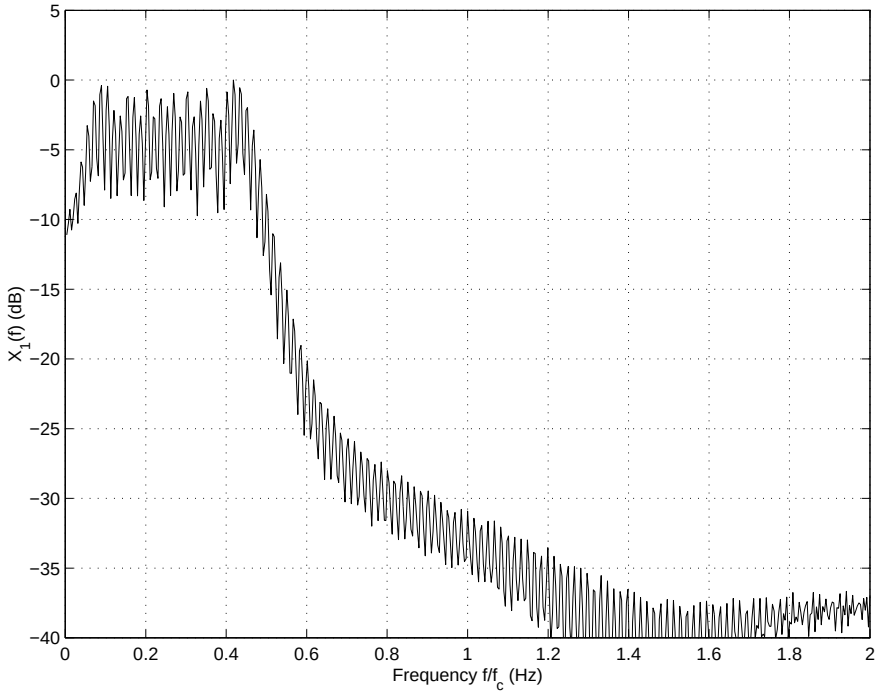

FIGURE 7.11: PSD of the in-phase branch at the transmitter after spreading of the data signal with the SSB complex unique combination spreading code C_1 (L=121,sps=4,r=1).

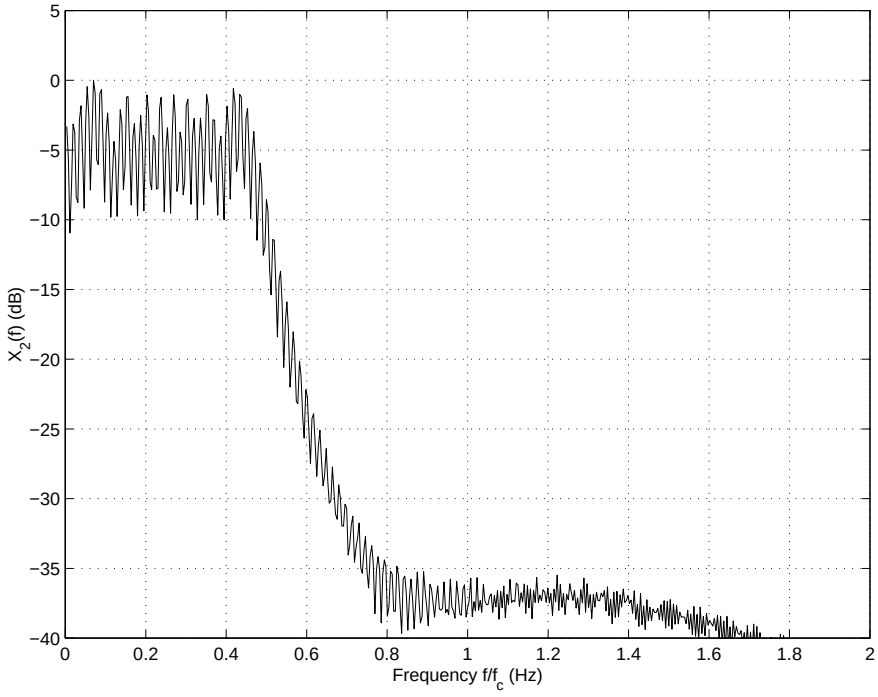

FIGURE 7.12: PSD of the quadrature-phase branch at the transmitter after spreading of the data signal with the SSB complex unique combination spreading code C_2 (L=121,sps=4,r=1).

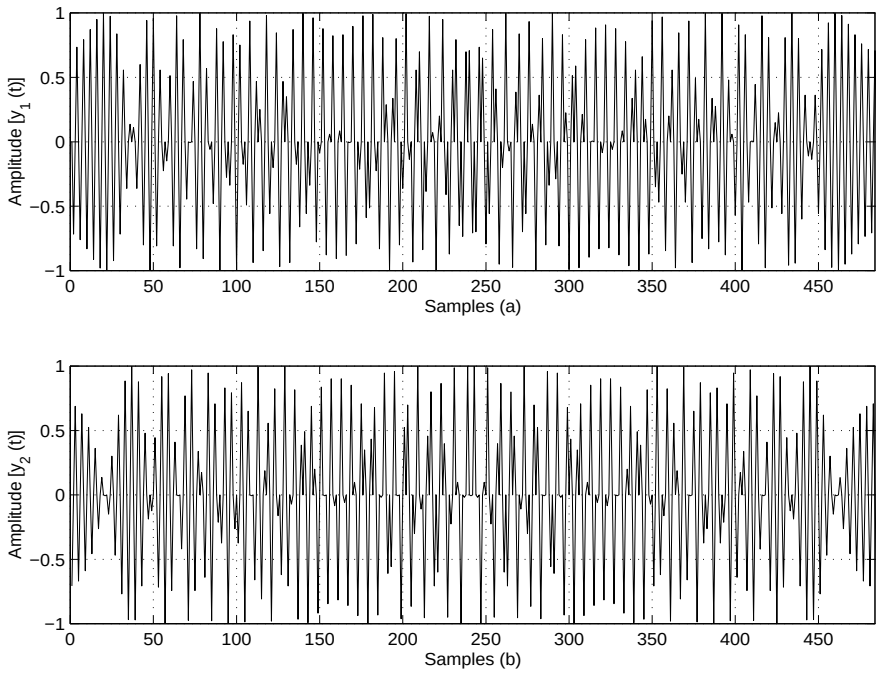

FIGURE 7.13: In-phase branch in (a) and quadrature phase branch in (b) at the transmitter after modulation of the DSB spreaded data signal onto the cosine and sine carriers, respectively (L=121,sps=4,r=1).

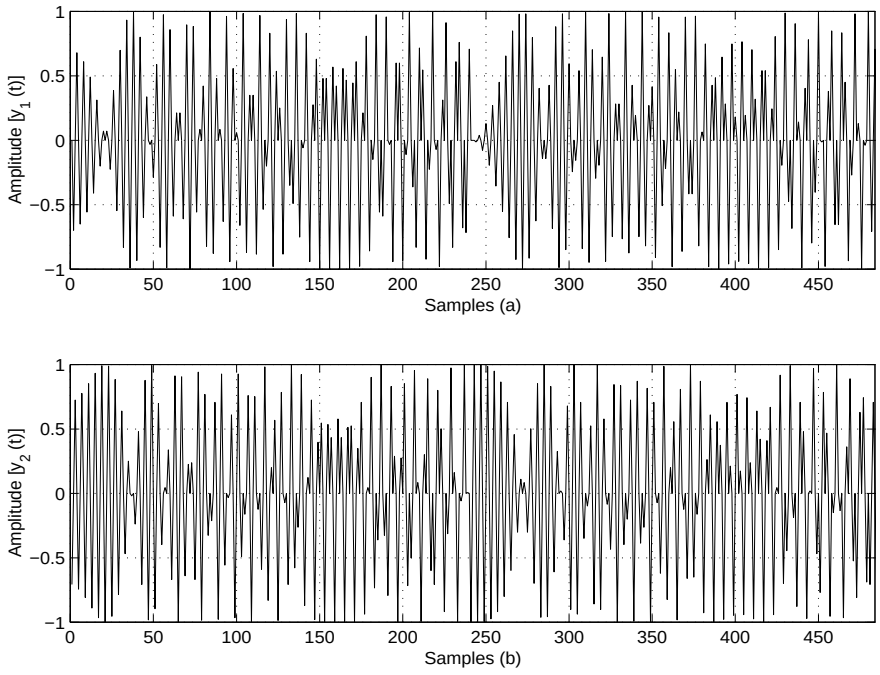

FIGURE 7.14: In-phase branch in (a) and quadrature phase branch in (b) at the transmitter after modulation of the SSB spreaded data signal onto the cosine and sine carriers, respectively (L=121,sps=4,r=1).

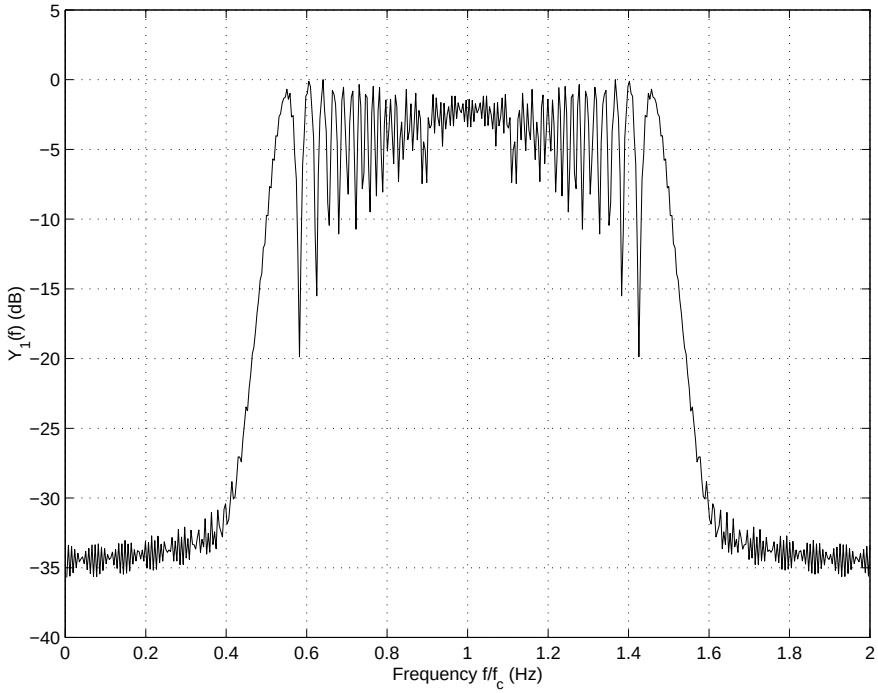

FIGURE 7.15: PSD of the in-phase branch at the transmitter after modulation of the DSB spreaded data signal onto the cosine carrier (L=121,sps=4,r=1).

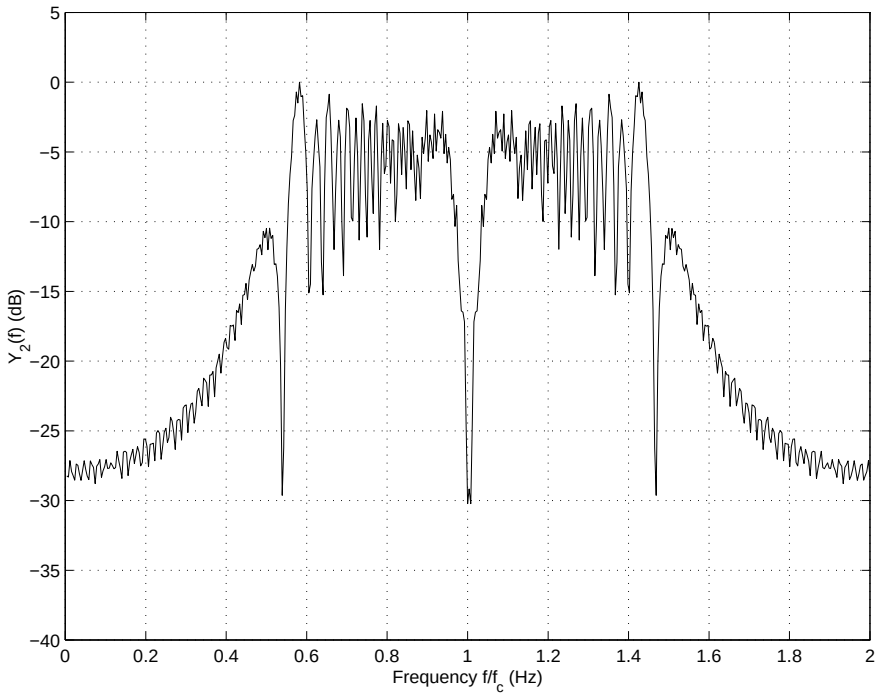

FIGURE 7.16: PSD of the quadrature phase branch at the transmitter after modulation of the DSB spreaded data signal onto the sine carrier (L=121,sps=4,r=1).

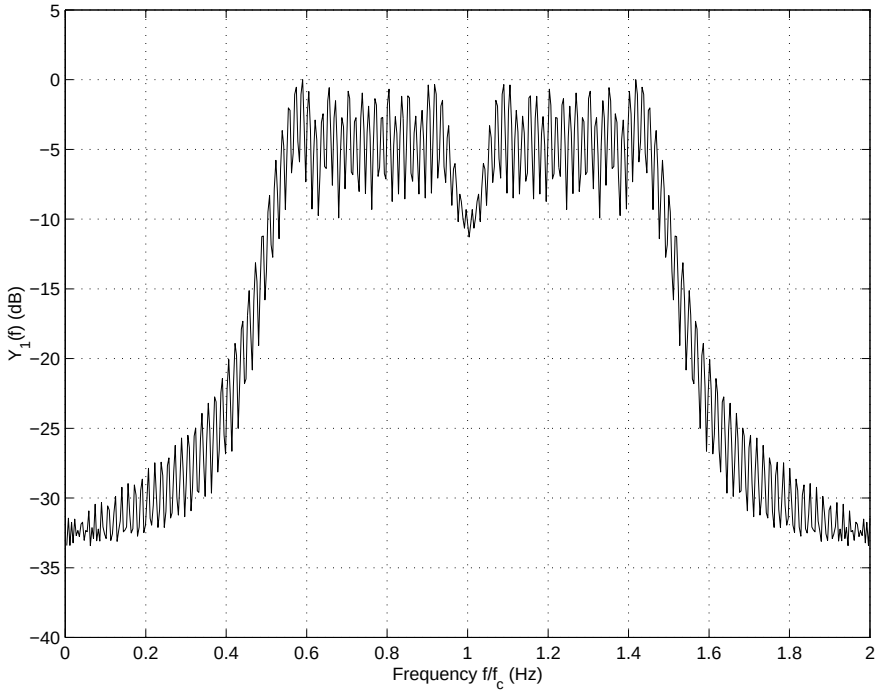

FIGURE 7.17: PSD of the in-phase branch at the transmitter after modulation of the SSB spreaded data signal onto the cosine carrier (L=121,sps=4,r=1).

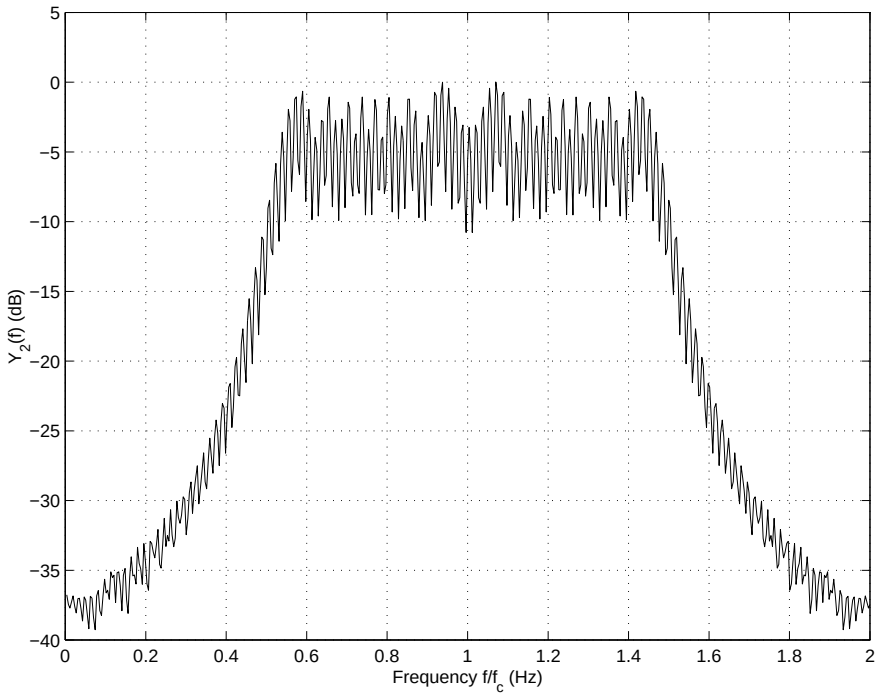

FIGURE 7.18: PSD of the quadrature phase branch at the transmitter after modulation of the SSB spreaded data signal onto the sine carrier (L=121,sps=4,r=1).

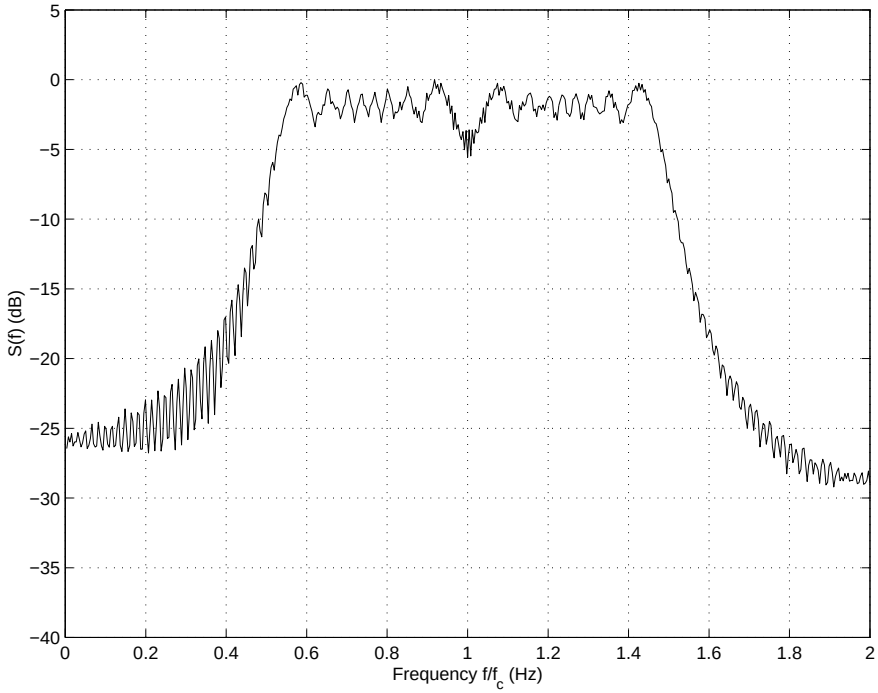

FIGURE 7.19: PSD of the final output of the DSSS transmitter when using DSB CSS in the case of balanced and QPSK (L=121,sps=4,r=1)

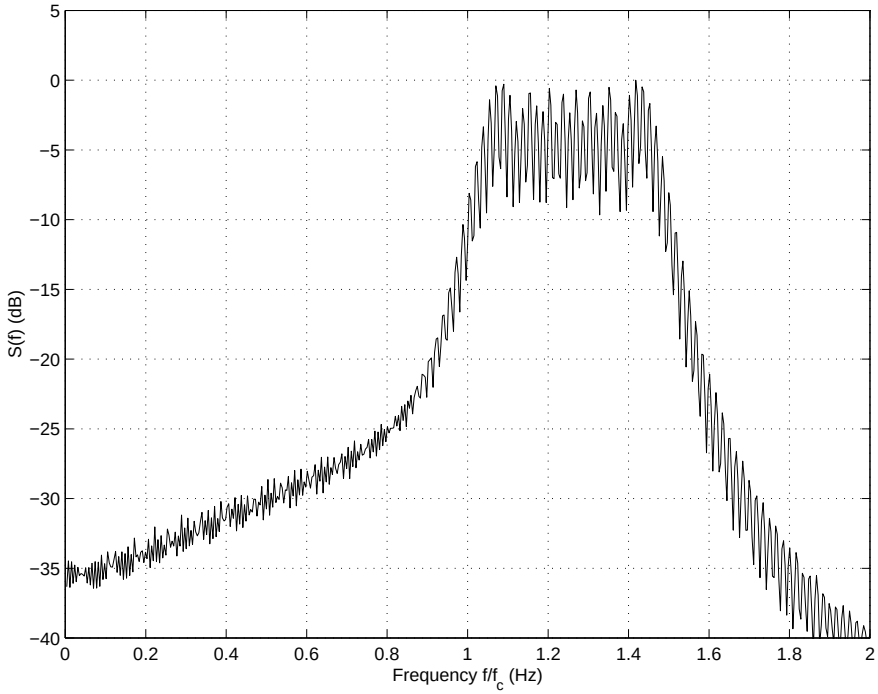

FIGURE 7.20: PSD of the final output of the DSSS transmitter when using SSB CSS in the case of balanced QPSK (L=121,sps=4,r=1)

CHAPTER EIGHT

SIMULATION OF THE DSSS RECEIVER

8.1 INTRODUCTION AND DESCRIPTION

The theoretically analysed DSSS receiver structures, which form the complete complex DSSS system, have been simulated in C++. Figure 7.1 presents a block diagram of the complete simulated system. The simulation of the receiver with all corresponding results are presented in this chapter. Figure 8.1 shows the block diagram of the receiver for the case of the balanced QPSK as well as the normal QPSK configuration. The receiver consists of two multipliers in parallel, despreading the incoming signal with the receiver's replica of spreading codes C_1 and C_2, which are the same synchronized unique combinations used in the transmitter, provided by the VCCG module in the complex DLL subsystem. These despreaded signals are then demodulated with the recovered quadrature sine and cosine carriers and then integrate-and-dumped to produce $g_1(t)$ and $g_2(t)$, respectively. For the case of the balanced QPSK configuration, $g_(t)$ and $g_2(t)$ are summed and sampled, whereafter a decision is made to recover the original data. For the dual channel QPSK configuration, the two parallel signals, $g_1(t)$ and $g_2(t)$, are sampled separately, whereupon decisions are made based on these samples, in order to recover the original two data streams. The following figures will illustrate the signals at different points throughout the receiver structure for both configurations, as well as for the cases where DSB and SSB CSS are used in the spreading and despreading processes.

The decision-directed complex Costas carrier recovery loop, decision-directed complex DLL as well as the acquisition circuitry are also simulated to perform a fully independent receiver structure responsible for code acquisition, carrier recovery and code tracking.

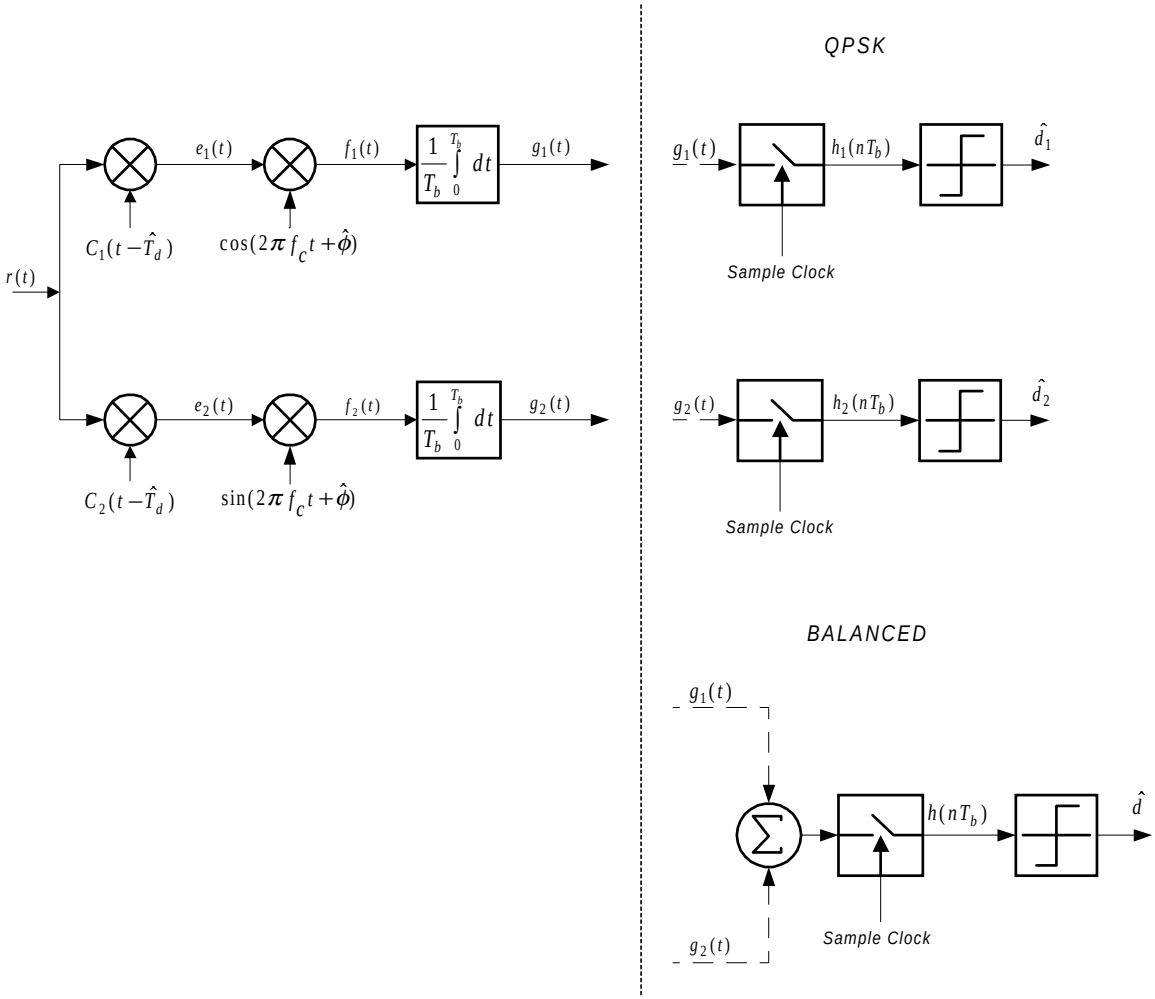

FIGURE 8.1: Block diagram of the receiver structure used in the simulation

Results related to these loop structures will also be given in this chapter.

8.2 SIMULATION RESULTS AND DISCUSSION

The two branch signals after despreading, $e_1(t)$ and $e_2(t)$, are shown in Figure 8.2 for the case of DSB CSS and Figure 8.3 shows the case for SSB CSS. The spectra for these despreaded signals are shown in Figures 8.4 and 8.5 for the DSB CSS and in Figures 8.6 and 8.7 for SSB CSS. It can be seen in Figures 8.4, 8.5, 8.6 and 8.7 that the despreaded signals are still modulated onto the carrier signal and that the bandwidth is much narrower than that of the spreaded output signal at the transmitter. The recovered carriers, cosine and sine, are now used to demodulate the two branch signals to obtain $f_1(t)$ and $f_2(t)$, respectively, and is shown in Figure 8.8 for DSB CSS, and in Figure 8.9 for SSB CSS. The spectra for these despreaded demodulated signals are presented for DSB CSS in Figures 8.10 and 8.11 and in Figures 8.12 and 8.13 for SSB CSS. The length of the CSS, from which the unique despreading code combinations is generated, is $L = 121$, with 4 samples per chip and $r = 1$. In this case the processing gain of the system equald $10log(121) = 20.83dB$.

The in-phase and quadrature branch signals, after integrate-and-dump operation, are shown in Figure 8.14, for DSB CSS, while Figure 8.15 shows the case using SSB CSS. In the case of DSB CSS, the PSD of the in-phase branch signal is depicted in Figure 8.16 and for the quadrature branch in Figure 8.17. The PSDs for the in-phase and quadrature branch signals, using SSB CSS, are depicted in Figures 8.18 and 8.19, respectively.

In Figure 8.20 the PSD of the incoming signal, with $Eb/No = 10dB$, is shown, using DSB CSS, and in Figure 8.21 using SSB CSS. By despreading these signals with the unique spreading sequence combination C_1 in the case of DSB CSS, a PSD is obtained as show in Figure 8.22, and with unique combination C_2 the PSD shown in Figure 8.23 is obtained. When the SSB CSS input signal is despread with the unique combinations C_1 and C_2, respectively, the PSD of the in-phase branch is as depicted in Figure 8.24 and the PSD of the quadrature branch as in Figure 8.25, with $Eb/No = 10dB$.

Figure 8.26 shows the in-phase and quadrature branch signal after integrate-and-dump operation in the case of DSB CSS and at $Eb/No = 10dB$, while Figure 8.27 shows the integrate-and-dump output of the in-phase and quadrature branches when using SSB CSS.

The PSD of the incoming signal, with $Eb/No = 20dB$, is shown in Figure 8.28 when using DSB CSS. Figures 8.29 and 8.30 depicts the PSDs of the incoming signal with a $Eb/No = 30dB$, for the DSB and SSB cases, respectively.

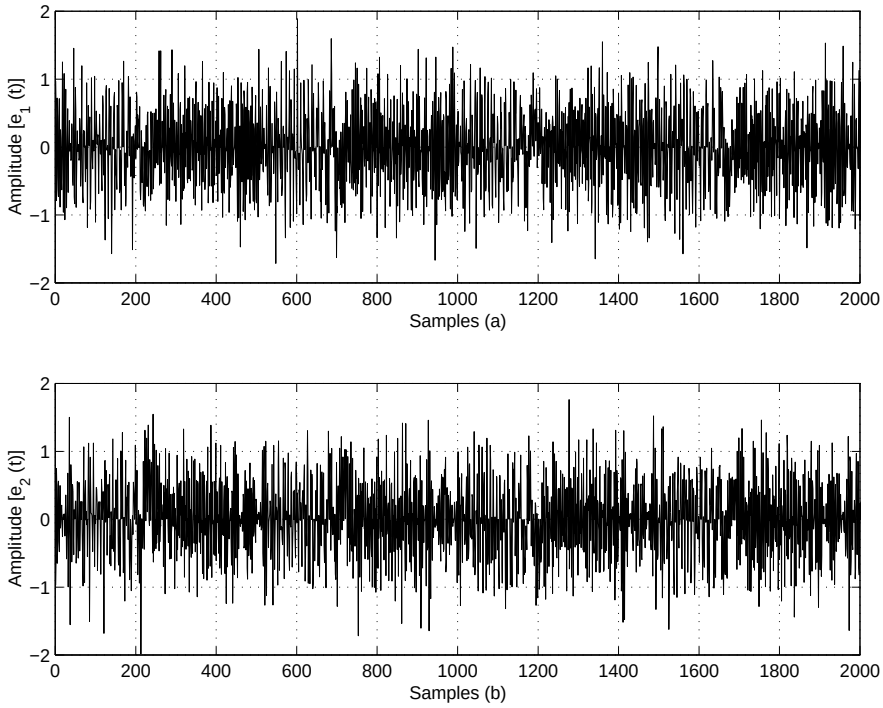

FIGURE 8.2: Incoming signal despreaded with unique combination C_1 in (a) and with C_2 in (b) for the case of DSB CSS (L=121, sps=4 and r=1).

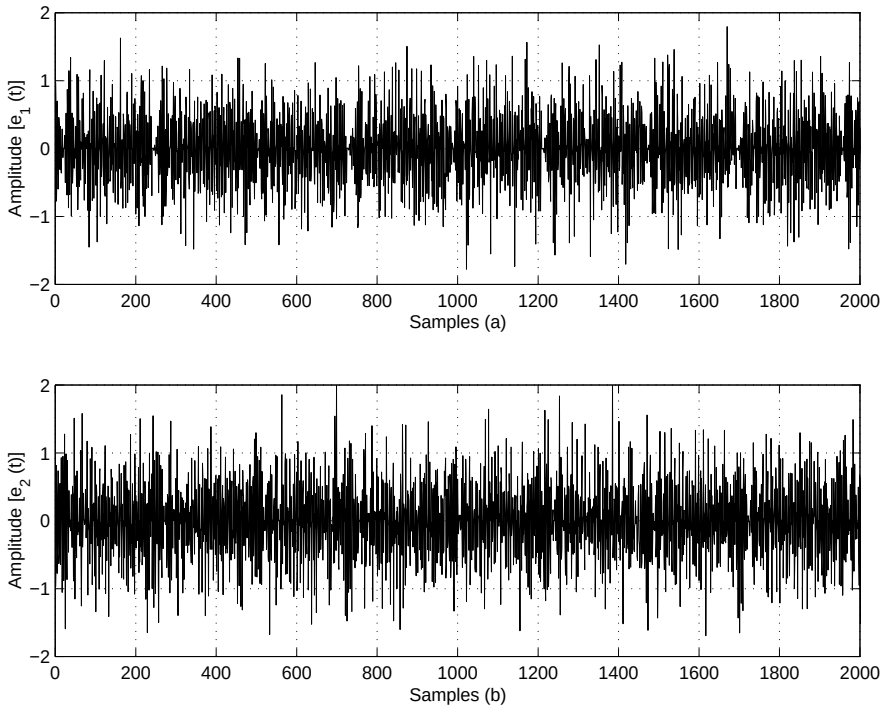

FIGURE 8.3: Incoming signal despreaded with unique combination C_1 in (a) and with C_2 in (b) for the case of SSB CSS (L=121, sps=4 and r=1).

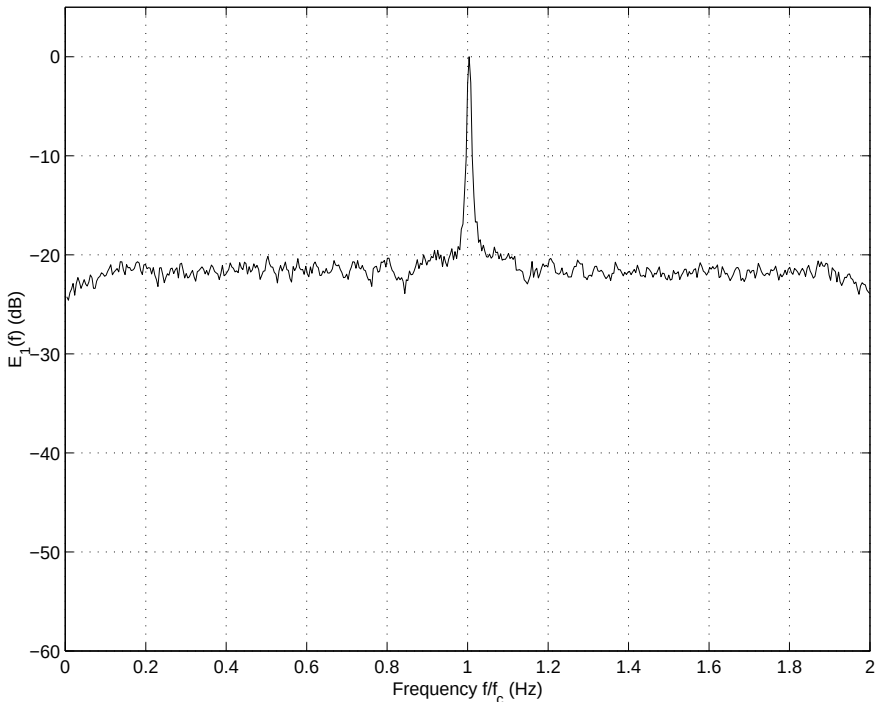

FIGURE 8.4: PSD of the incoming signal despreaded with the unique combination C_1 for the case of DSB CSS (L=121, sps=4 and r=1).

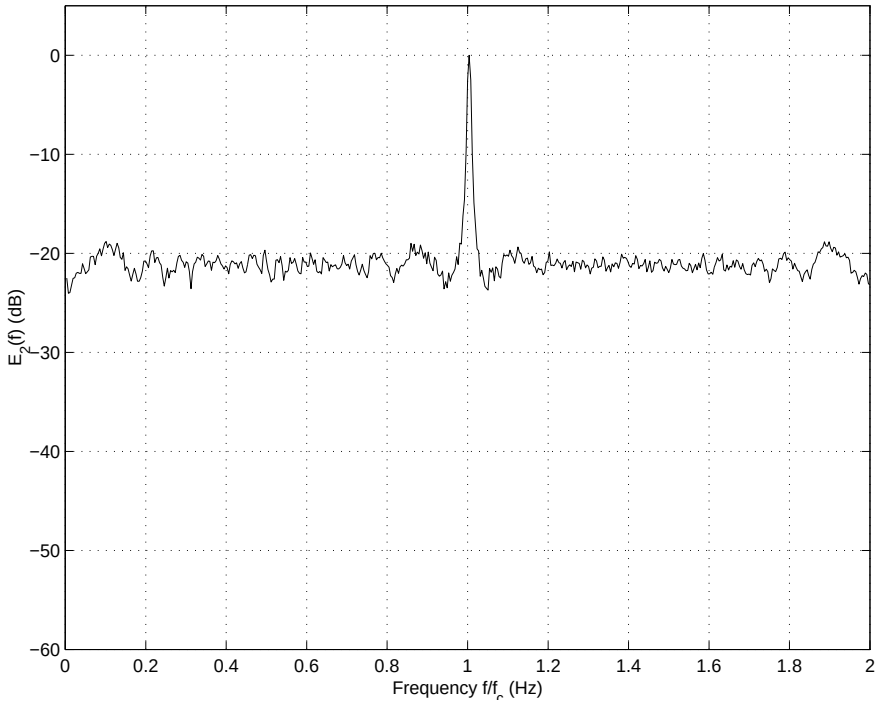

FIGURE 8.5: PSD of the incoming signal despreaded with the unique combination C_2 for the case of DSB CSS (L=121, sps=4 and r=1).

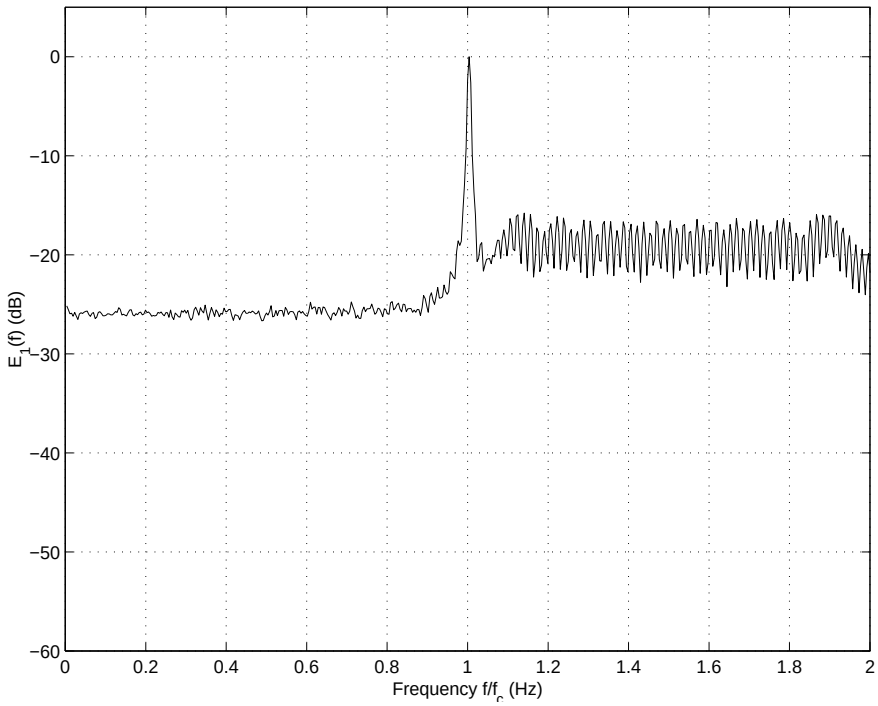

FIGURE 8.6: PSD of the incoming signal despreaded with the unique combination C_1 for the case of SSB CSS (L=121, sps=4 and r=1).

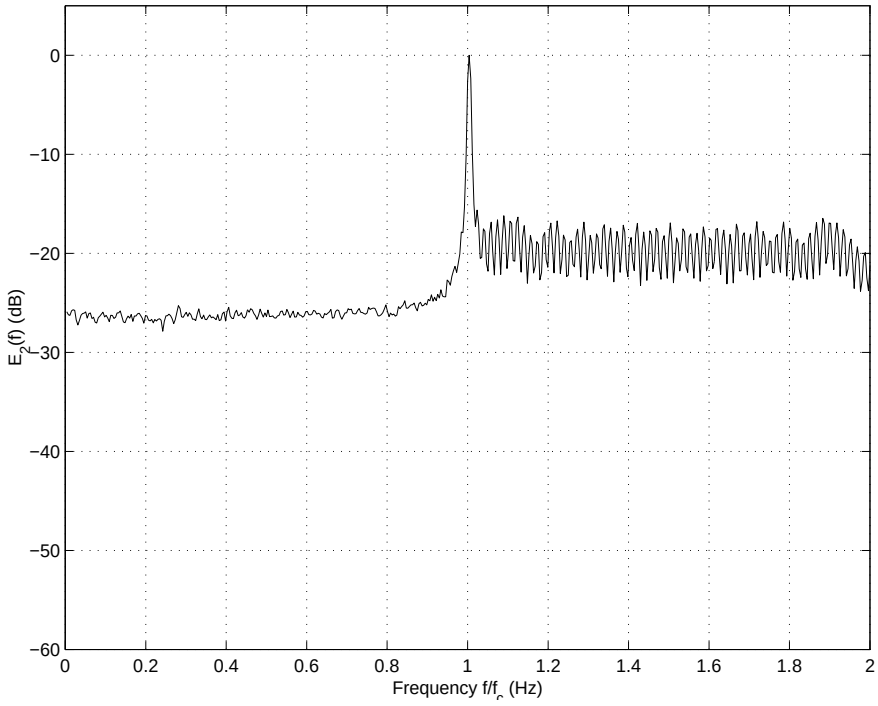

FIGURE 8.7: PSD of the incoming signal despreaded with the unique combination C_2 for the case of SSB CSS (L=121, sps=4 and r=1).

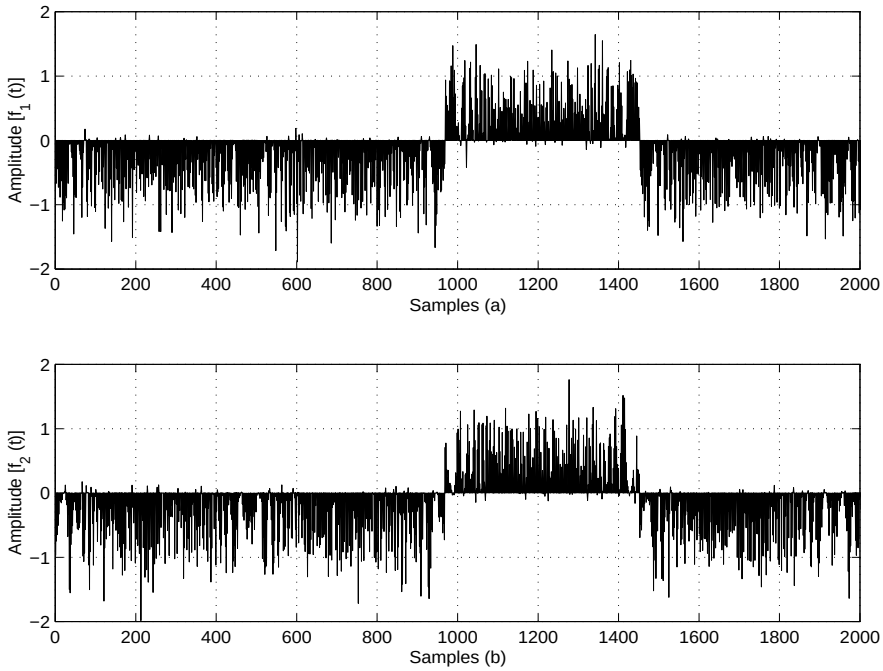

FIGURE 8.8: In-phase branch signal after despreading with DSB CSS C_1 and demodulation with the recovered cosine carrier in (a) and quadrature phase branch signal after despreading with DSB CSS C_2 and demodulation with the recovered sine carrier in (b) (L=121,sps=4,r=1).

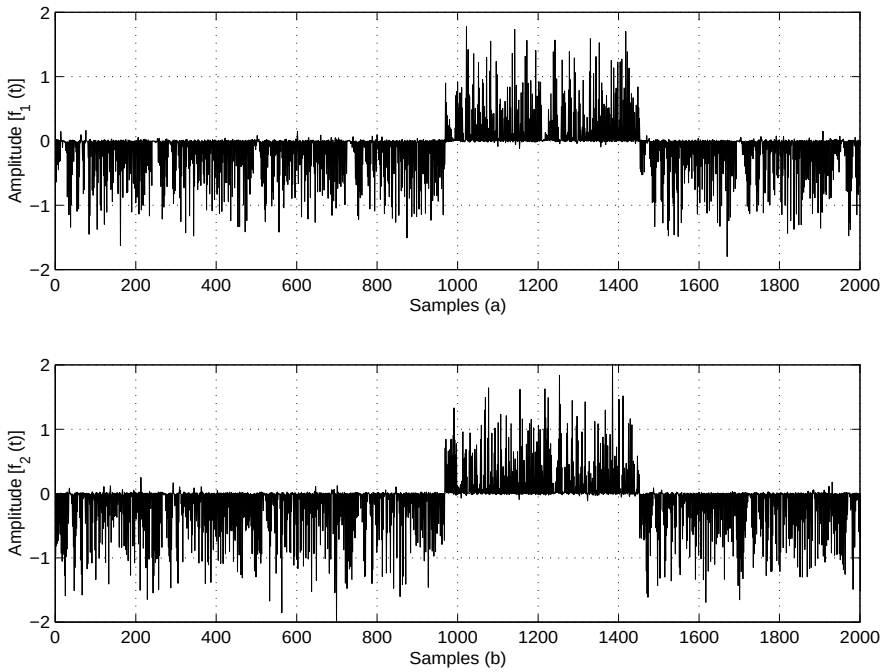

FIGURE 8.9: In-phase branch signal after despreading with SSB CSS C_1 and demodulation with the recovered cosine carrier in (a) and quadrature phase branch signal after despreading with SSB CSS C_2 and demodulation with the recovered sine carrier in (b) (L=121,sps=4,r=1).

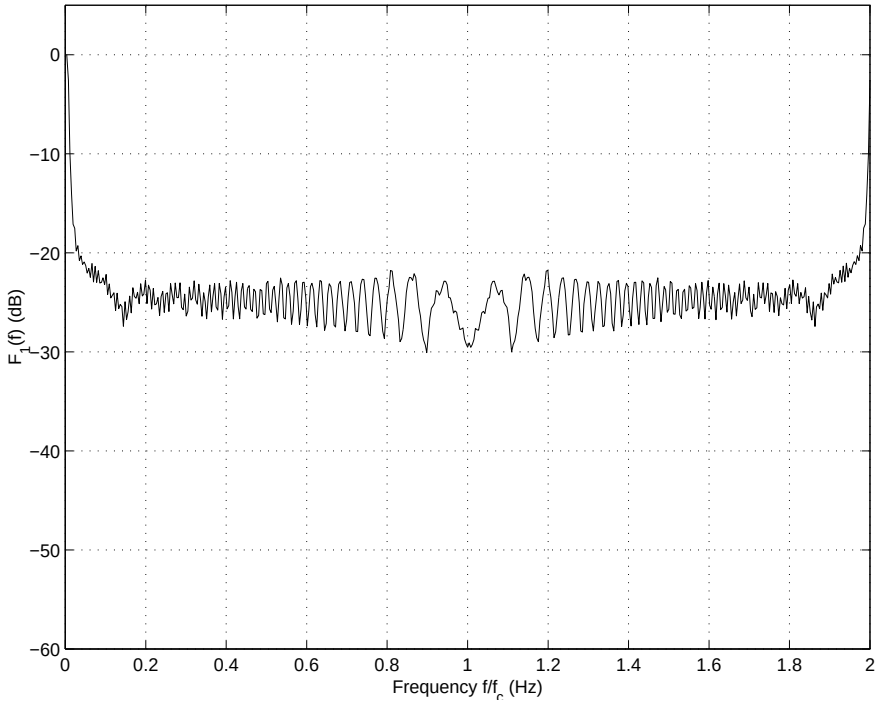

FIGURE 8.10: PSD of the in-phase branch signal after despreading with DSB CSS C_1 and demodulation with the recovered cosine carrier (L=121,sps=4,r=1).

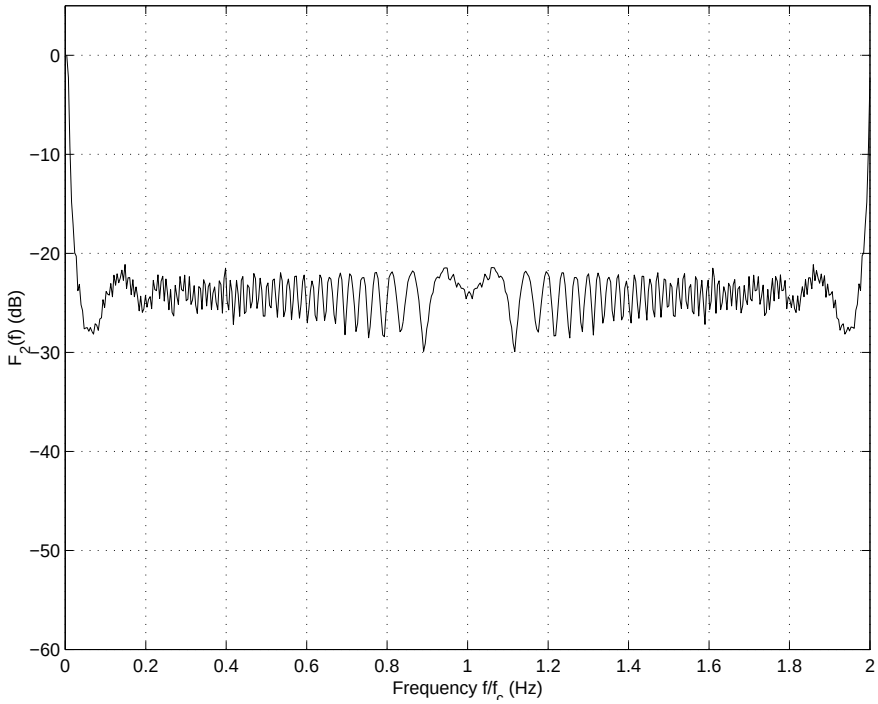

FIGURE 8.11: PSD of the quadrature phase branch signal after despreading with DSB CSS C_2 and demodulation with the recovered sine carrier (L=121,sps=4,r=1).

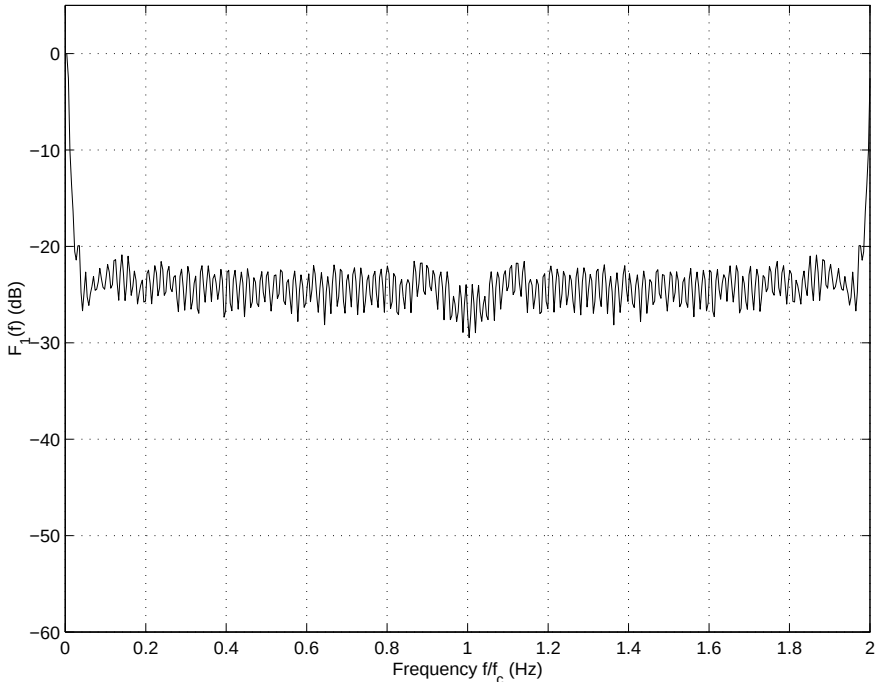

FIGURE 8.12: PSD of the in-phase branch signal after despreading with SSB CSS C_1 and demodulation with the recovered cosine carrier (L=121,sps=4,r=1).

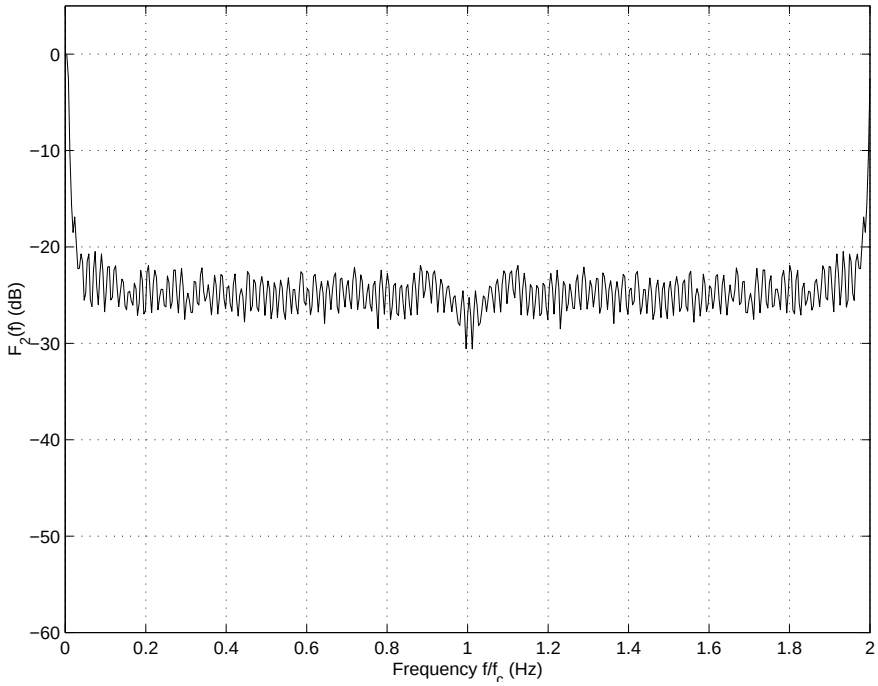

FIGURE 8.13: PSD of the quadrature phase branch signal after despreading with SSB CSS C_2 and demodulation with the recovered sine carrier (L=121,sps=4,r=1).

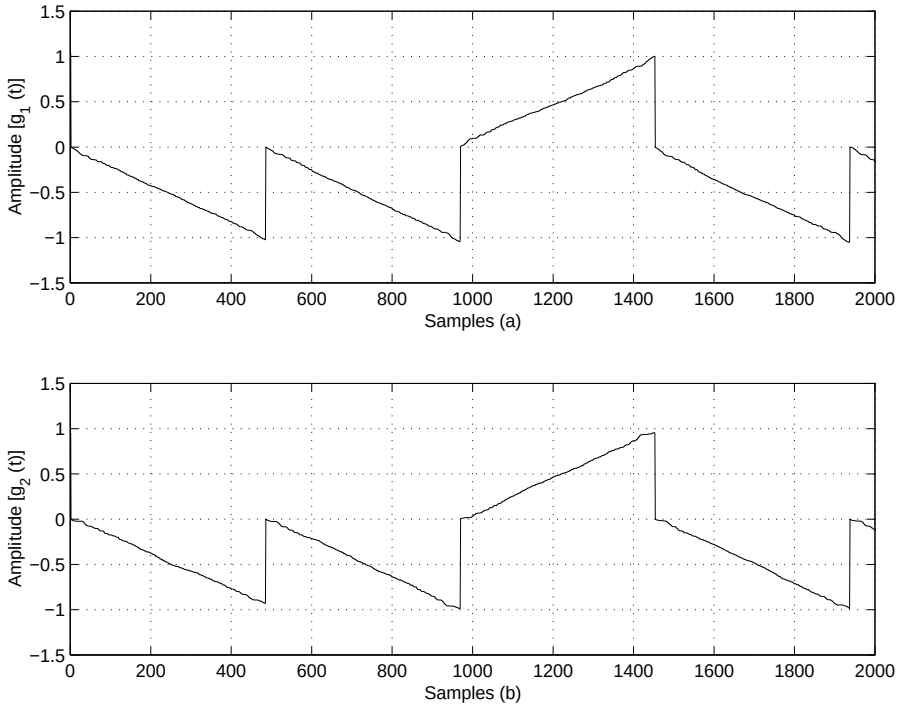

FIGURE 8.14: In-phase branch signal after integrate-and-dump operation in (a) and quadrature phase branch signal after integrate-and-dump operation in (b) for the case of DSB CSS.

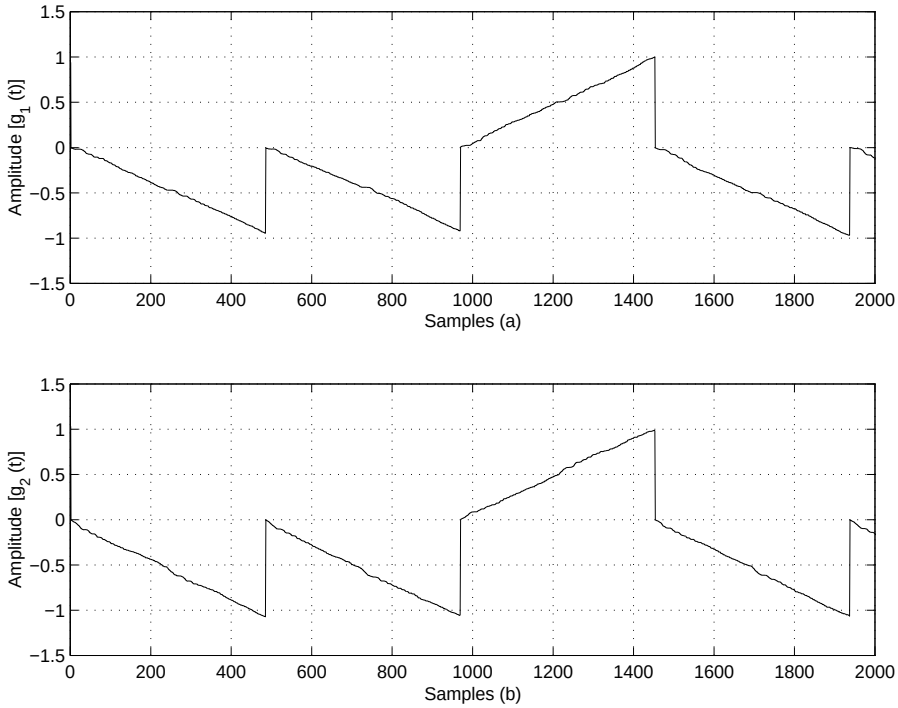

FIGURE 8.15: In-phase branch signal after integrate-and-dump operation in (a) and quadrature phase branch signal after integrate-and-dump operation in (b) for the case of SSB CSS.

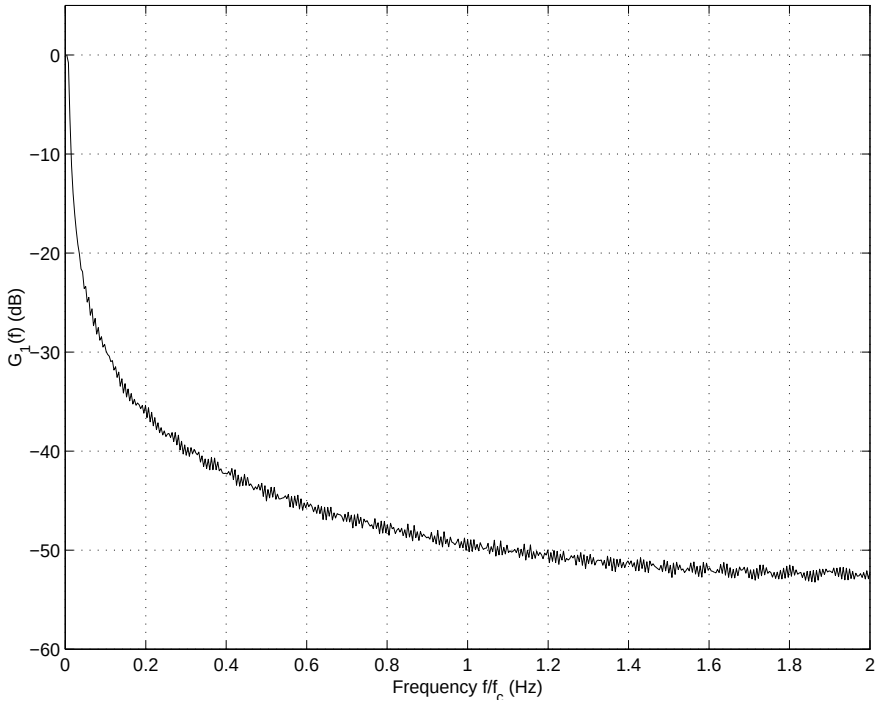

FIGURE 8.16: PSD of the in-phase branch signal after integrate-and-dump operation for the case of DSB CSS.

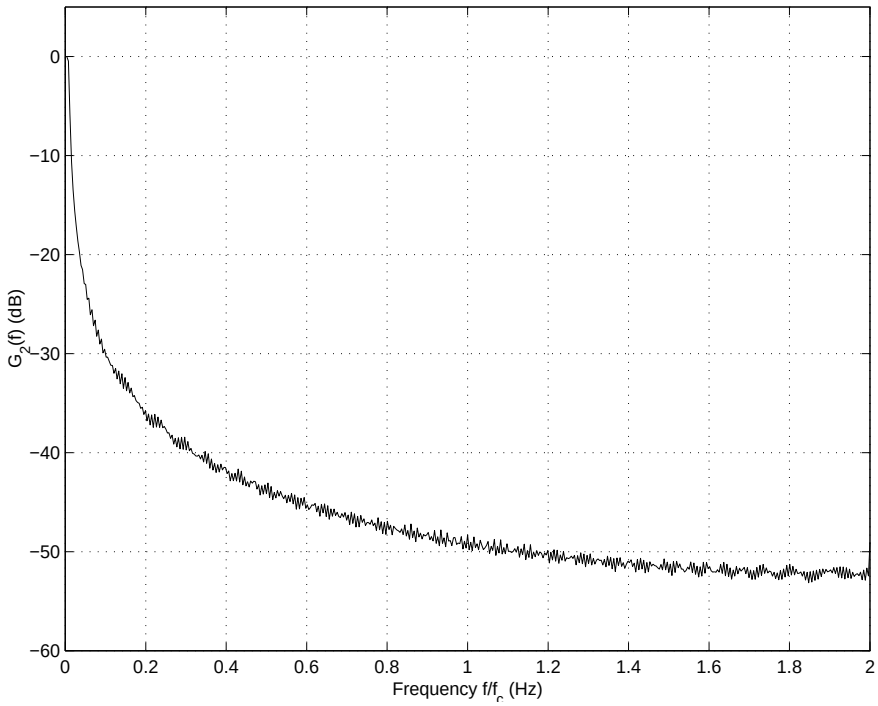

FIGURE 8.17: PSD of the quadrature phase branch signal after integrate-and-dump operation for the case of DSB CSS.

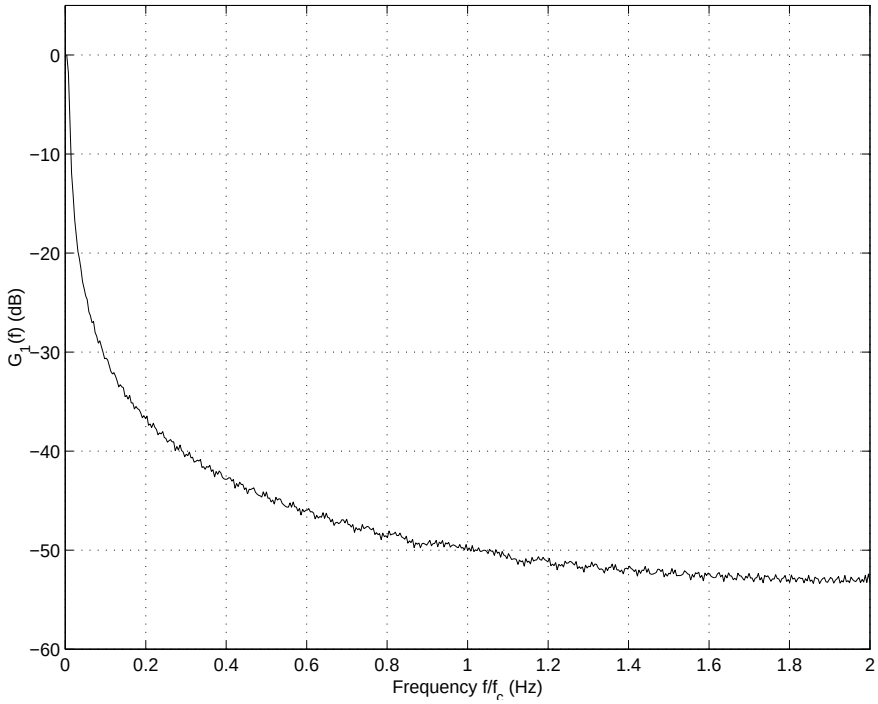

FIGURE 8.18: PSD of the in-phase branch signal after integrate-and-dump operation for the case of SSB CSS.

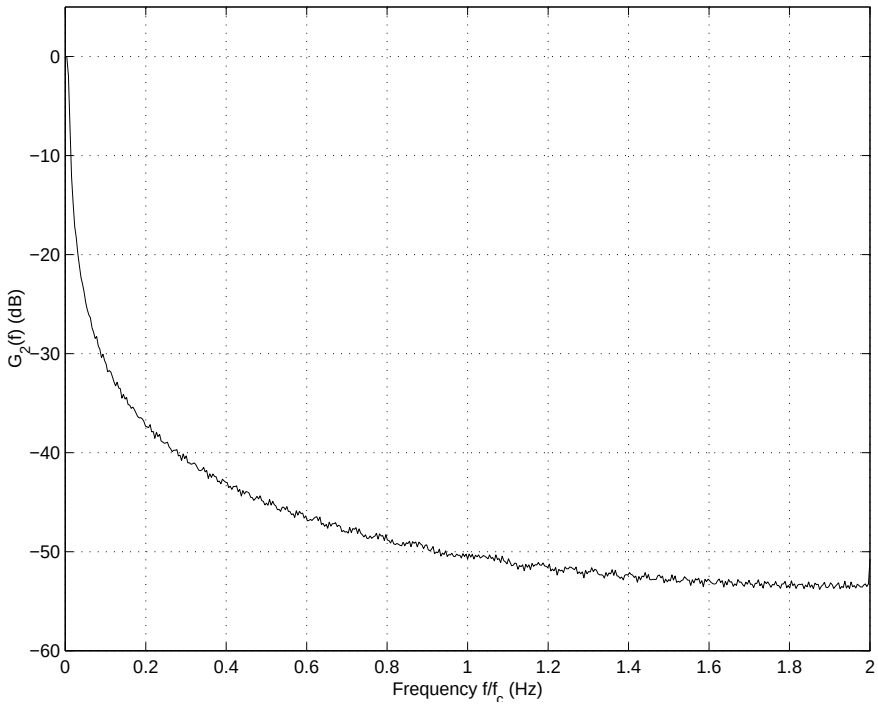

FIGURE 8.19: PSD of the quadrature phase branch signal after integrate-and-dump operation for the case of SSB CSS.

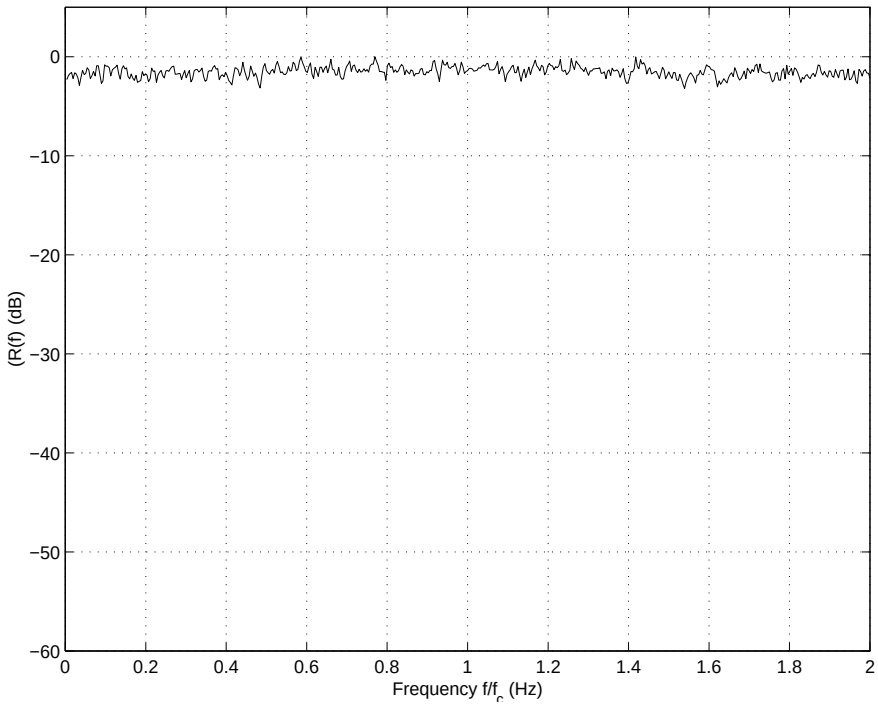

FIGURE 8.20: PSD of the incoming signal with a $Eb/No = 10dB$ and by using DSB CSS, (L=121,sps=4,r=1)

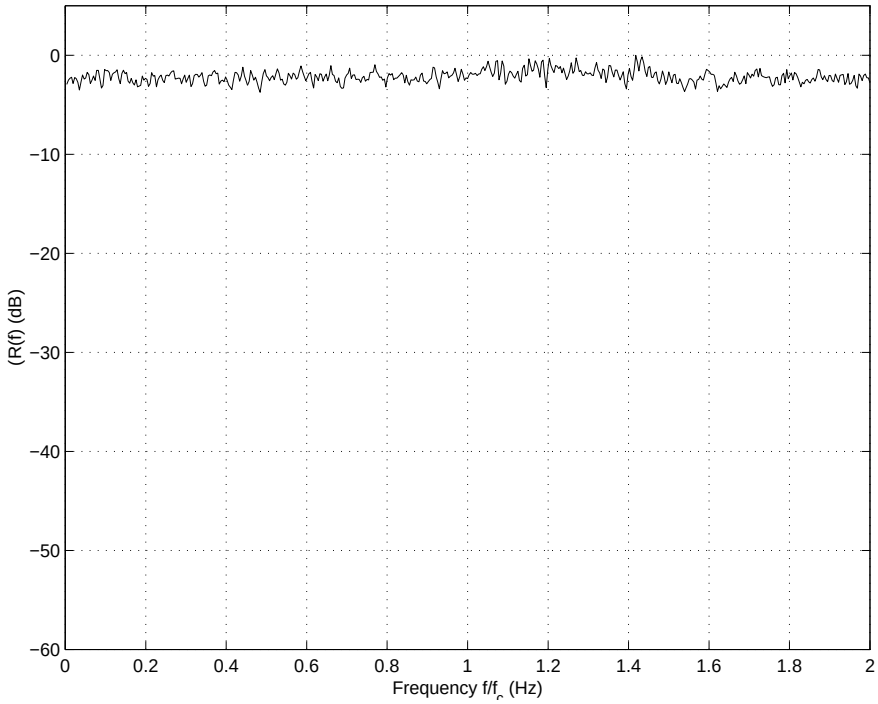

FIGURE 8.21: PSD of the incoming signal with a $Eb/No = 10dB$ and by using SSB CSS, (L=121,sps=4,r=1)

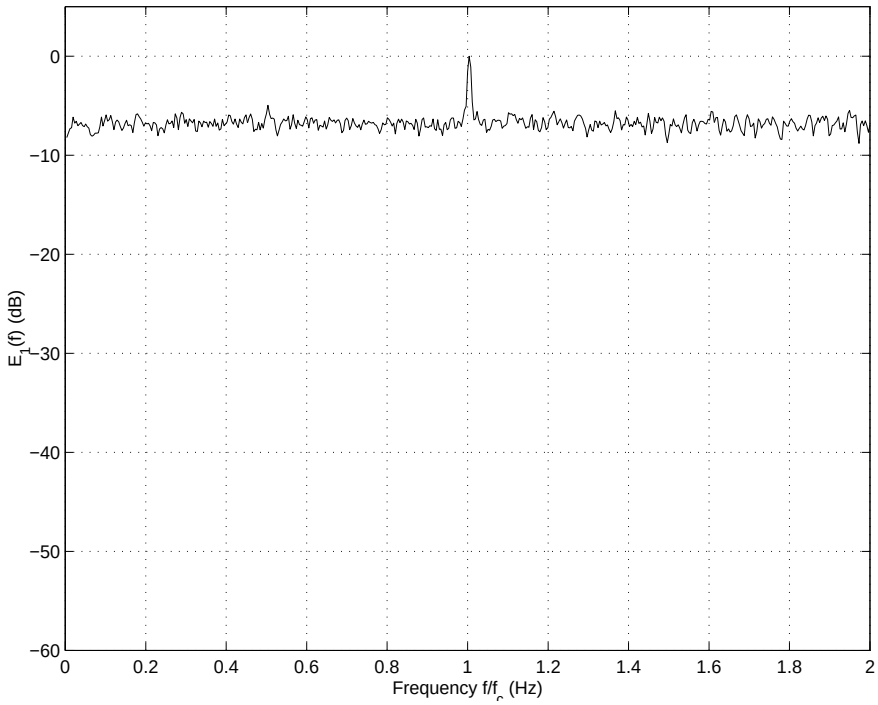

FIGURE 8.22: PSD of the incoming signal despreaded with the unique combination C_1 for the case of DSB CSS and at a $Eb/No = 10dB$, (L=121, sps=4 and r=1).

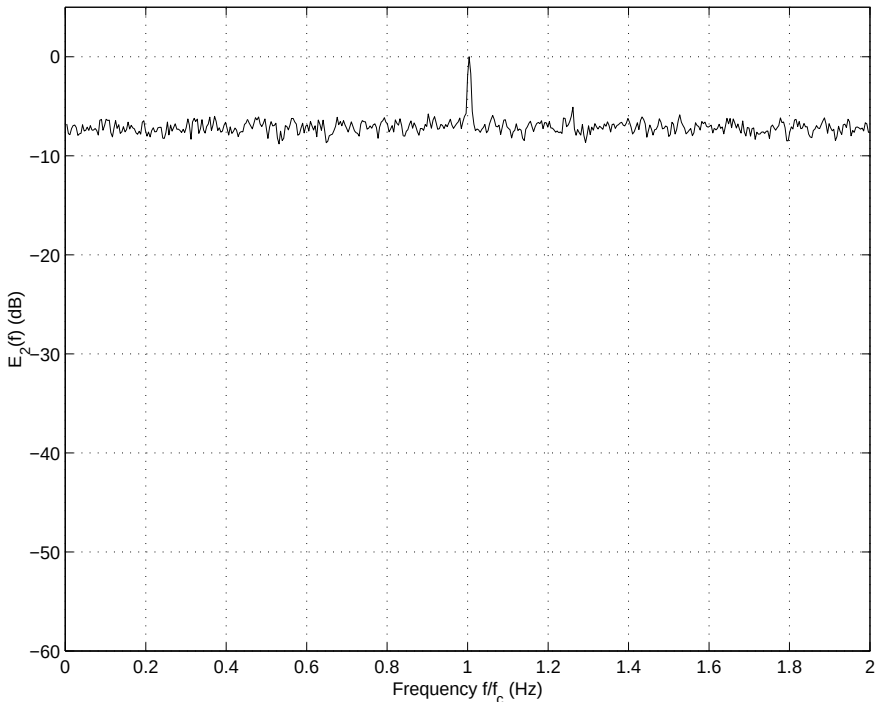

FIGURE 8.23: PSD of the incoming signal despreaded with the unique combination C_2 for the case of DSB CSS and at a $Eb/No = 10dB$, (L=121, sps=4 and r=1).

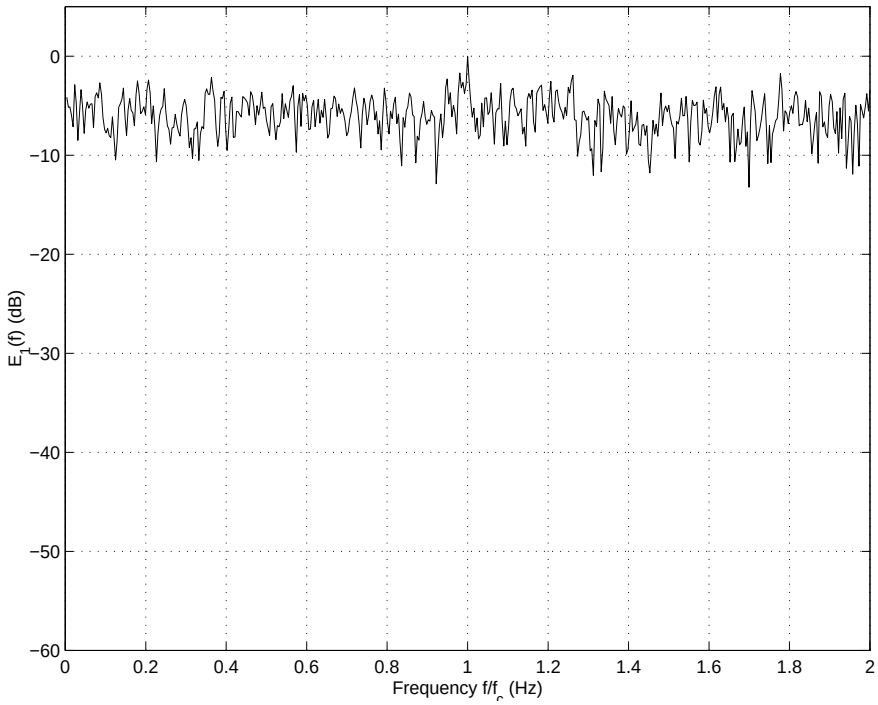

FIGURE 8.24: PSD of the incoming signal despreaded with the unique combination C_1 for the case of SSB CSS and at a $Eb/No = 10dB$, (L=121, sps=4 and r=1)

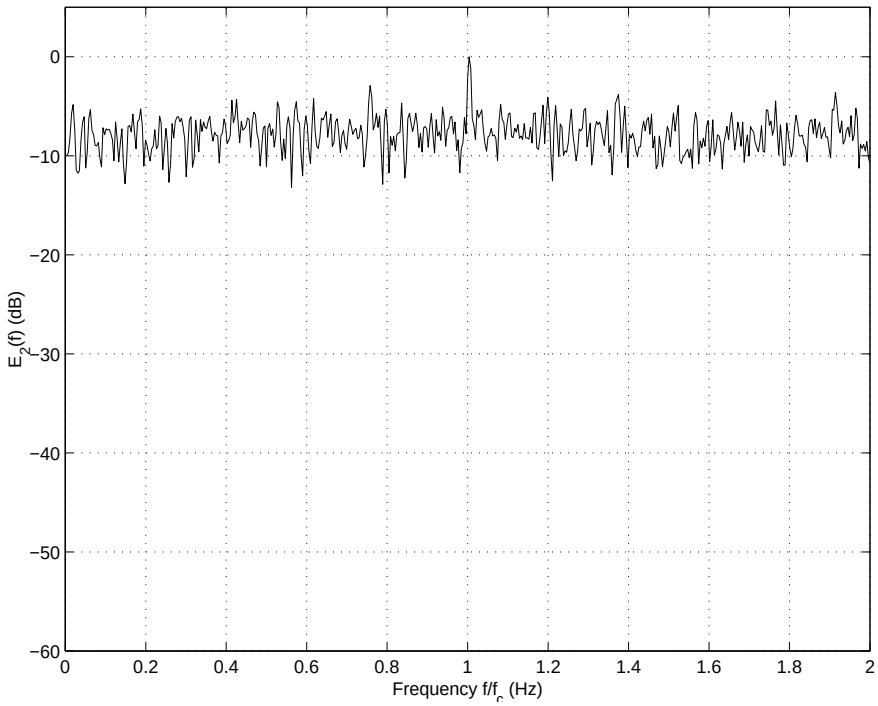

FIGURE 8.25: PSD of the incoming signal despreaded with the unique combination C_2 for the case of SSB CSS and at a $Eb/No = 10dB$, (L=121, sps=4 and r=1)

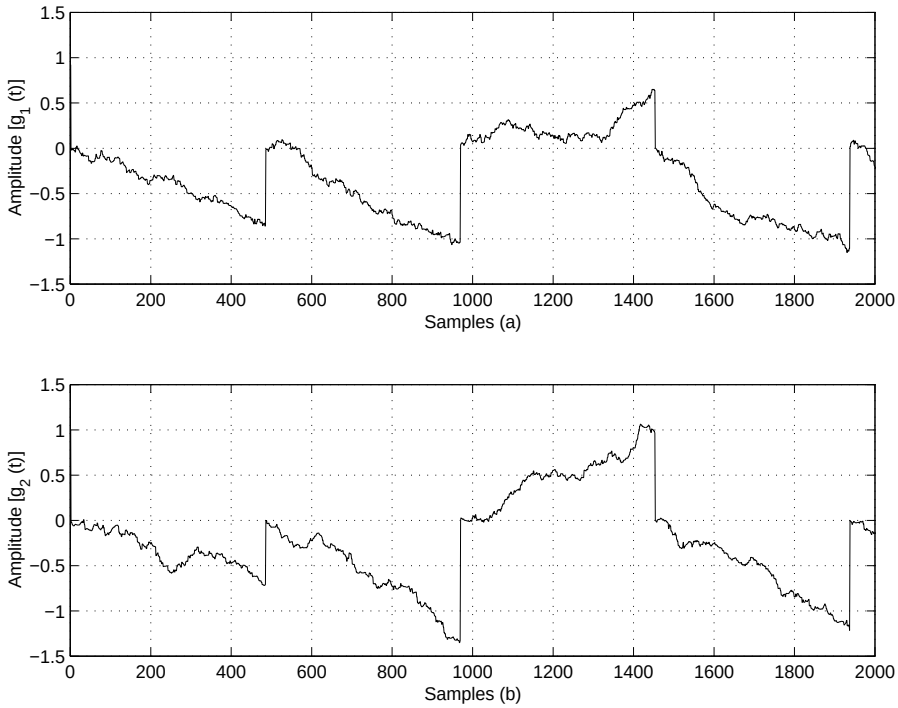

FIGURE 8.26: In-phase branch signal after integrate-and-dump operation in (a) and quadrature phase branch signal after integrate-and-dump operation in (b) for the case of DSB CSS and at $Eb/No = 10dB$, (L=121, sps=4 and r=1).

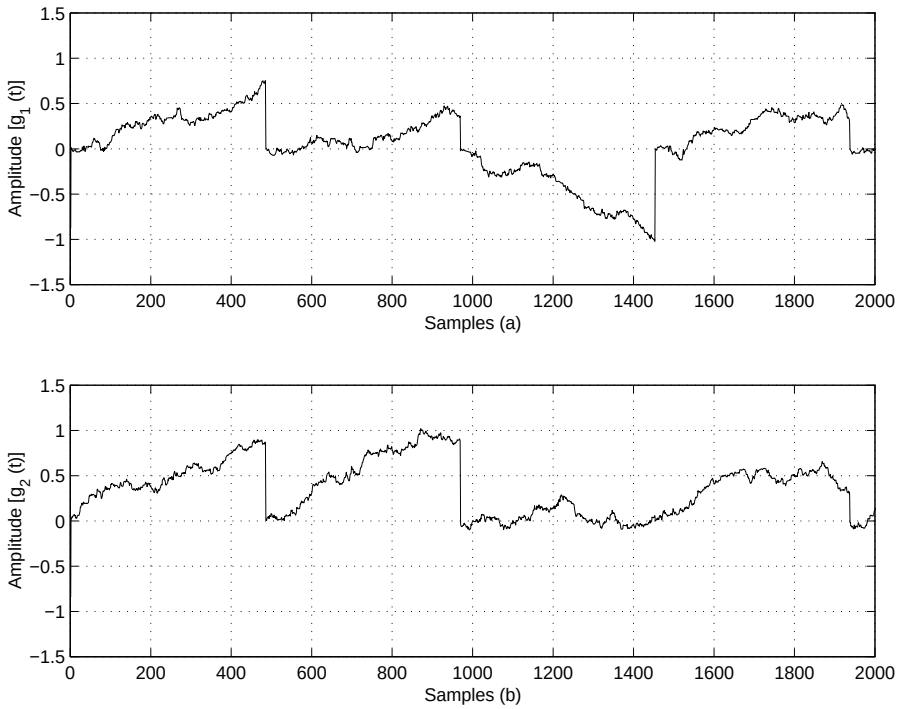

FIGURE 8.27: In-phase branch signal after integrate-and-dump operation in (a) and quadrature phase branch signal after integrate-and-dump operation in (b) for the case of SSB CSS and at $Eb/No = 10dB$, (L=121, sps=4 and r=1).

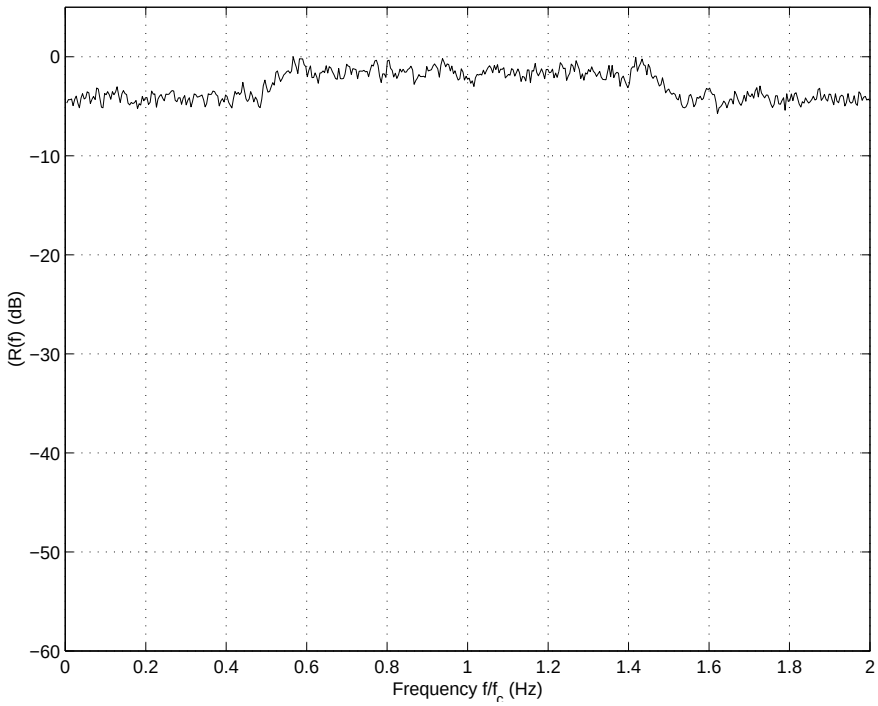

FIGURE 8.28: PSD of the incoming signal with a $Eb/No = 20dB$ and by using DSB CSS, with L=121, sps=4 and r=1

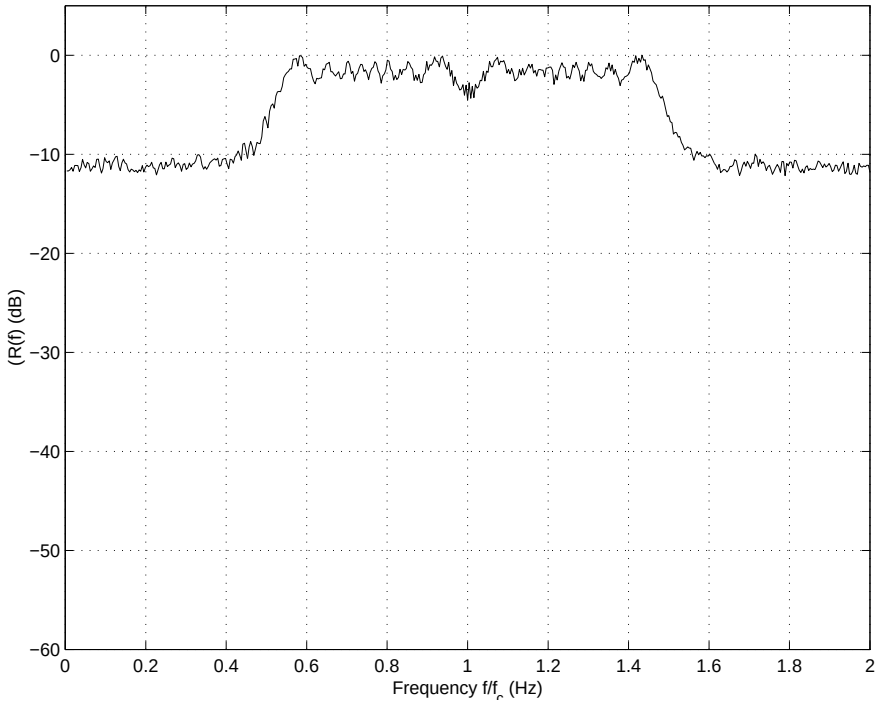

FIGURE 8.29: PSD of the incoming signal with a $Eb/No = 30dB$ and by using DSB CSS, with L=121, sps=4 and r=1

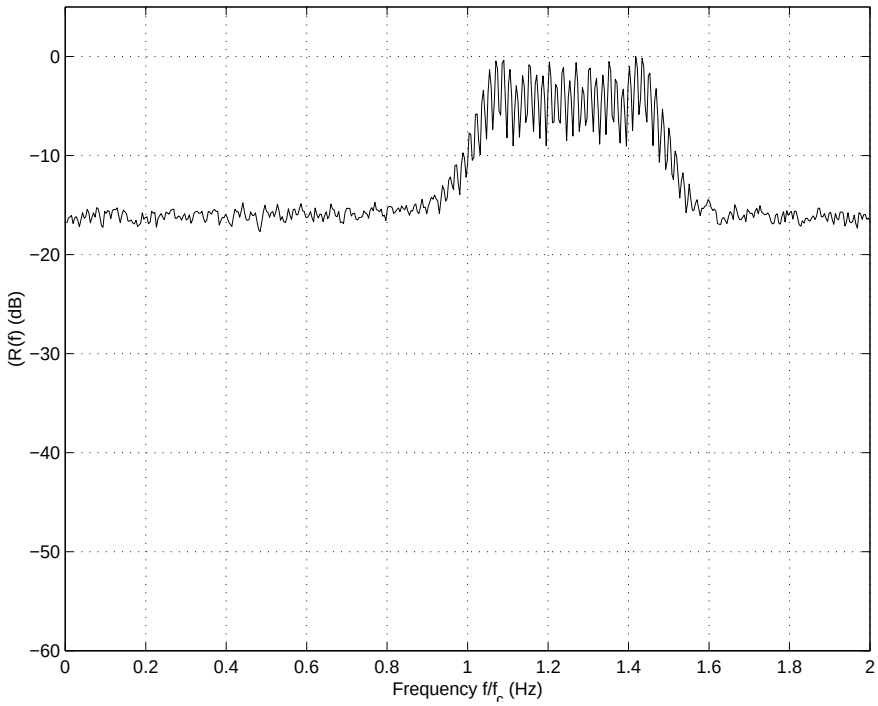

FIGURE 8.30: PSD of the incoming signal with a $Eb/No = 30dB$ and by using SSB CSS, with L=121, sps=4 and r=1